

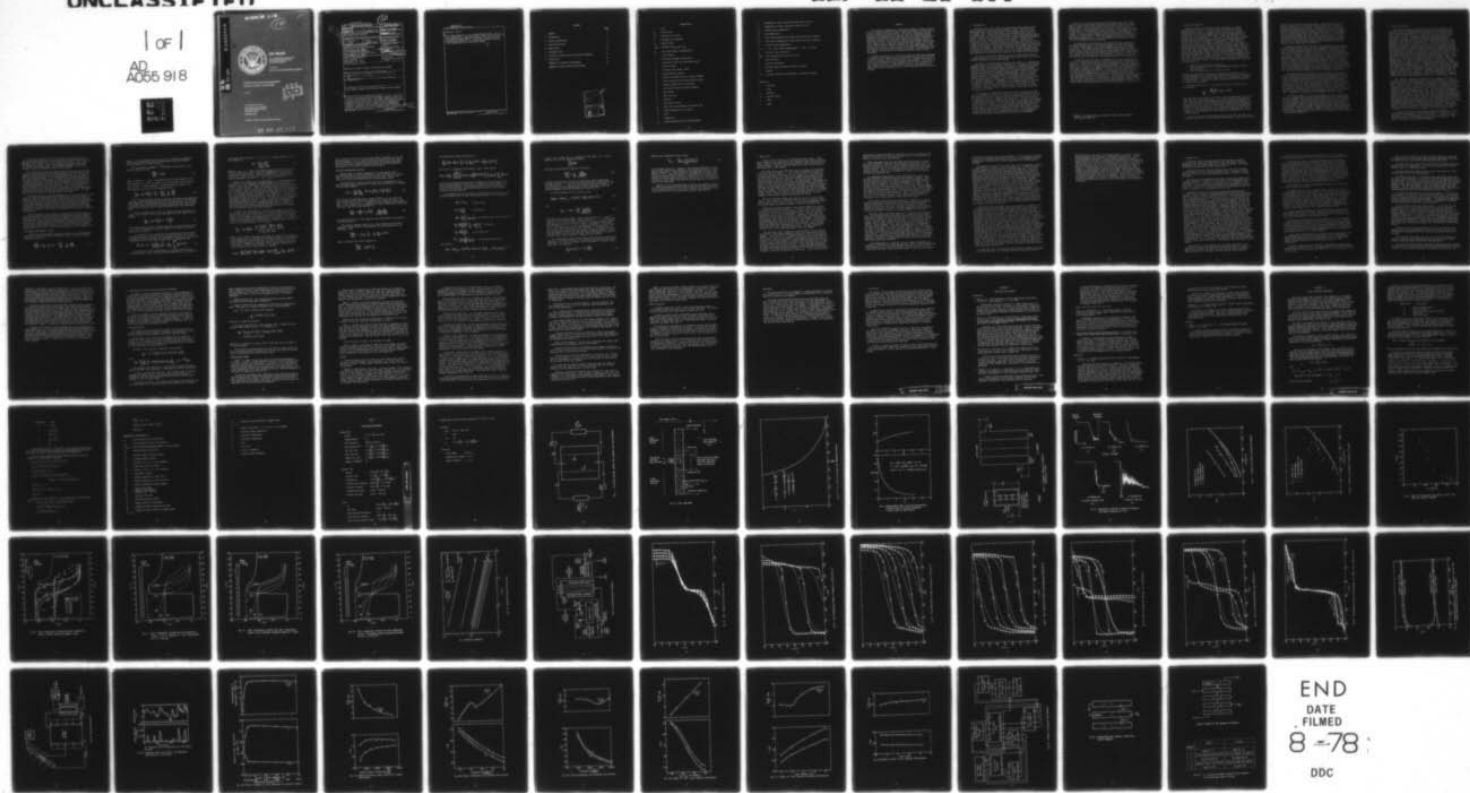
AD-A055 918

COLORADO STATE UNIV FORT COLLINS DEPT OF MECHANICAL --ETC F/6 10/3
THERMAL STRATIFICATION ENHANCEMENT FOR SOLAR ENERGY APPLICATION--ETC(U)
JUL 77 R I LOEHRKE, M K SHARP, H N GARI N68305-76-C-0036

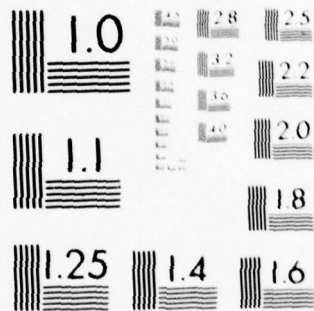
UNCLASSIFIED

1 of 1

AD
A055 918



END
DATE
FILMED
8-78
DDC



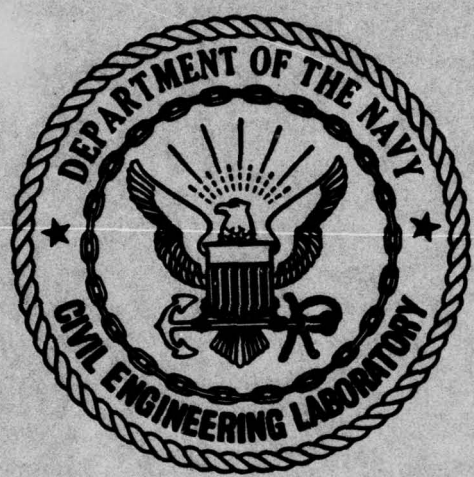
MICROCOPY RESOLUTION TEST CHART
NATIONAL BUREAU OF STANDARDS-1963-A

FOR FURTHER TRAN *top secret*

12

AD A055918

AD No. _____
DDC FILE COPY



CR 78.011

CIVIL ENGINEERING LABORATORY
Naval Construction Battalion Center
Port Hueneme, California

Sponsored by
NAVAL FACILITIES ENGINEERING COMMAND

**THERMAL STRATIFICATION ENHANCEMENT
FOR SOLAR ENERGY APPLICATIONS**

July 1977

DDC
RECEIVED
JUL 5 1978
F

An Investigation Conducted by
COLORADO STATE UNIVERSITY
Mechanical Engineering Department
Fort Collins, Colorado
N68305-76-C-0036

Approved for public release; distribution unlimited.

78 06 27 103

UNCLASSIFIED

SECURITY CLASSIFICATION OF THIS PAGE (When Data Entered)

19 REPORT DOCUMENTATION PAGE		READ INSTRUCTIONS BEFORE COMPLETING FORM
1. REPORT NUMBER CR-78.011	2. GOVT ACCESSION NO.	3. RECIPIENT'S CATALOG NUMBER
4. TITLE (and Subtitle) THERMAL STRATIFICATION ENHANCEMENT FOR SOLAR ENERGY APPLICATIONS.		5. TYPE OF REPORT & PERIOD COVERED Final report
6. AUTHOR(s) R. I./Loehrke M. K./Sharp		7. PERFORMING ORG. REPORT NUMBER
8. PERFORMING ORGANIZATION NAME AND ADDRESS Colorado State University Mechanical Engineering Department Fort Collins, CO 80523		9. CONTRACT OR GRANT NUMBER(s) N68305-76-C-0036
10. CONTROLLING OFFICE NAME AND ADDRESS Civil Engineering Laboratory Naval Construction Battalion Center Port Hueneme, CA 93043		11. PROGRAM ELEMENT, PROJECT, TASK AREA & WORK UNIT NUMBERS 62765N; ZF57.571.001.01.010
12. MONITORING AGENCY NAME & ADDRESS (if different from Controlling Office) Chief of Naval Material Navy Department Washington, DC 20360		13. REPORT DATE Jul 1977
14. SECURITY CLASS. (of this report) Unclassified		15. NUMBER OF PAGES 79
16. DISTRIBUTION STATEMENT (of this Report) Approved for public release; distribution unlimited.		17. SECURITY CLASS. (of this report) Unclassified
18. DISTRIBUTION STATEMENT (of the abstract entered in Block 20, if different from Report) F57571 ZF57571 461		19. SUPPLEMENTARY NOTES
20. KEY WORDS (Continue on reverse side if necessary and identify by block number) Solar energy, thermal stratification, thermal solar storage		
21. ABSTRACT (Continue on reverse side if necessary and identify by block number) A study is presented that shows methods to enhance stratification in liquid storage tanks. The report focusses on the development of a passive inlet distributor which minimizes mixing between incoming and stored fluids at unlike temperatures. Theoretical analyses and scale model tests were performed. Computer simulations were used to compare mixed storage with		

DD FORM 1 JAN 73 1473 EDITION OF 1 NOV 65 IS OBSOLETE

UNCLASSIFIED

SECURITY CLASSIFICATION OF THIS PAGE (When Data Entered)

405570

78 06 27 103

act

UNCLASSIFIED

SECURITY CLASSIFICATION OF THIS PAGE (When Data Entered)

Block 20. Cont'd

stratified storage in a solar space heating system. Test results showed that in some cases nearly ideal stratification can be obtained and the computer simulations indicated that the load carrying capability of a solar system may be increased 5-10% through the use of stratified storage.

UNCLASSIFIED

SECURITY CLASSIFICATION OF THIS PAGE (When Data Entered)

Contents

	<u>Page</u>
Summary	i
1. Introduction	1
2. Design Considerations	3
3. Inlet Distributors	5
4. Model Tests	13
5. Prototype Tests	17
6. Effects of Stratification on System Performance	21
7. Conclusions	29
Appendix A, Annotated Bibliography	31
Appendix B, Ideal Stratified Tank Model	35

ACCESSION for	
NTIS	<input checked="" type="checkbox"/> File Section
DDC	<input type="checkbox"/> B. II Section
UNANNOUNCED	<input type="checkbox"/> []
JUSTIFICATION	
BY	
DISTRIBUTION/AVAILABILITY NOTES	
Dist	SPECIAL
A	

Nomenclature

A	- area
A_o	- orifice area
A_s	- surface area of tank
b	- thickness of insulation
c_p	- specific heat
C_{min}	- minimum of $\dot{m}_\ell c_{p\ell}$ and $\dot{m} c_{pr}$
C_D	- loss coefficient for perforations
D	- tank diameter
e	- load heat exchanger effectiveness
f	- fraction of total load supplied by solar
f	- friction factor
F_R	- collector heat removal factor
g	- acceleration of gravity
h	- height of incoming fluid in reaction chamber
H_T	- solar insolation on tilted collector surface
k_i	- thermal conductivity of insulation
K	- loss coefficient for manifold elements.
L	- tank height
\dot{m}	- mass flow rate
p	- pressure
q	- heat transfer rate
q_e	- heat loss to environment from storage tank
q_u	- useful energy gain in collector
t	- time
T	- temperature
T_a	- ambient temperature of tank environment

T_c - temperature of water supplied to tank from collector
 T_ℓ - temperature of water returning to tank from load
 T_{ref} - reference tank temperature
 T_r - room temperature
 T_{ri} - fluid inlet temperature on room side of load heat exchanger
 T_{ro} - fluid outlet temperature on room side of load heat exchanger
 T_s - average storage temperature
 T_1, T_2, \dots, T_N - tank segment temperatures, 1 - top, N - bottom.
 U_L - collector loss coefficient
 $(UA)_L$ - total conductance for heat loss load
 V - fluid velocity
 z - vertical coordinate
 Δz - vertical spacing between resistance elements
 ρ - density
 $(\tau\alpha)$ - collector effective transmittance - absorptance product

Subscripts

c - collector
 ℓ - load
 m - manifold
 mi - manifold inlet
 r - room
 t - tank

Summary

This study was undertaken to investigate methods to enhance stratification in liquid storage tanks and to assess the effects of stratification on the performance of solar systems. The study of enhancement methods focussed on the development of a passive inlet distributor which would minimize mixing between incoming and stored fluids at unlike temperatures. Theoretical analyses and scale model tests were performed to evaluate distributor designs. Final tests in a 600 gallon prototype storage tank with a porous, vertical manifold revealed that nearly ideal stratification can be achieved under conditions in which the inlet temperatures to the storage tank are fixed. Under variable inlet temperature conditions less than perfect stratification was generally realized. The theoretical work has, however, pointed the way to improved performance under variable conditions.

Computer simulations of a solar, space heating system were performed to contrast the performance using mixed storage with that using perfectly stratified storage. Many simulations were run to determine the effect of certain system parameters on the comparative performance. The results of this study, along with a single comparison found in the literature for a water heating application, show that the load carrying capability of a solar system may be increased from 5 to 10% through the use of stratified storage.

1. Introduction

Effective use of solar energy for heating and cooling requires that thermal energy be stored for varying periods of time. The most widely used method simply stores heated water in an insulated tank in the form of sensible heat. Studies have indicated that thermal stratification in the storage tank can increase the efficiency of solar energy heating/cooling systems. There are several reasons for this increase in system performance; because of thermal stratification the surface water is hotter and the bottom water cooler than would otherwise be achieved. The hot water delivered to the load is therefore hotter than that obtained from unstratified storage and for example can be more efficiently used to operate an absorption system air conditioner. The cooler bottom water, on the other hand, is sent to the solar collector to be heated. Since solar collectors operate more efficiently at low temperatures this use of "cool" water increases the net heat absorbed by the collector over that from an unstratified storage tank.

The purpose of the work reported here was to investigate techniques to enhance stratification in liquid storage tanks and to assess the possible economic advantages of stratified storage.

In order to facilitate the discussion of this work it is convenient to introduce certain classifications or definitions. Considering the possible methods by which heat may be added or removed from a storage tank one may define as DIRECT those schemes in which hot and cold water are dumped directly into the tank and as INDIRECT those schemes in which hot and cold fluids pass through heat exchangers within the tank. Thus if hot water from the collector, or water heated by the collector fluid in a heat exchanger external to the storage tank, is introduced into the tank the storage system would be DIRECT. On the other hand if the collector fluid were passed through a coil submerged in the storage tank the storage system would be INDIRECT. Furthermore, if no external energy is required to enhance stratification within the tank the storage system will be classified as PASSIVE while if external energy is required, for example to control a thermally selective valving system, the storage system will be classified as ACTIVE.

It is taken for granted that the coolest water in the storage tank will be withdrawn to supply the collector, or the heat exchanger removing heat from the collector fluid, and that the warmest water in the tank will be supplied to the load. However, the condition of the water returning to the storage tank will depend on the application. For those applications in which the return water is maintained at the storage temperature extremes (collector water at least as hot as the warmest storage water and makeup water as least as cold as the coolest storage water) the operating conditions will be called FIXED indicating that the location within the tank at which these flows should be introduced is fixed. If the temperatures of the incoming flows may lie anywhere within the storage temperature extremes the operating conditions will be referred to as VARIABLE.

Almost all of the work reported in the literature deals with DIRECT, PASSIVE stratification schemes operating under FIXED conditions. Experiments on natural circulation systems [1,3]* indicate stratification in storage tanks in which presumably the only special design feature is that the hot water is introduced at the top of the tank. Experiments on pumped systems [2,4,5,6] also indicate that stratification can be achieved. However, in one test under VARIABLE operating conditions the stratification was found to be minimal [2]. With the exception of reference [5] these experiments provide little in the way of generalized design data and none at all for VARIABLE operating conditions.

The theoretical work pertaining to stratified storage consists of a preliminary design analysis [8], computer models for stratified storage [7,9] and a single computer simulation comparing mixed and stratified storage [9]. The models, which apply to either DIRECT PASSIVE or DIRECT ACTIVE systems, have certain deficiencies (see annotated bibliography) which open to question some conclusions drawn from the simulations. These should not, however, significantly alter the estimated 6% increase in solar load carrying capacity attributable to stratified storage for one application [9].

Although the published data are limited, it is clear that stratification can be achieved using DIRECT, PASSIVE techniques under FIXED operating conditions. While FIXED conditions may be appropriate for certain applications, e.g. collector flow rate modulated to maintain a high exit temperature level and cold makeup water added to replace the hot water withdrawn, the most general conditions are VARIABLE. In fact, it may be that stratification will provide the biggest payoff in applications which inherently involve variable return temperatures such as in air conditioning applications. In any event control costs would be minimized if stratification could be achieved under VARIABLE conditions. Furthermore, it seems reasonable to anticipate that the stratified system of lowest overall cost would be a DIRECT, PASSIVE system capable of maintaining stratification under VARIABLE conditions. The focus of the research reported next was on the development of such a system.

* Numbers in brackets refer to references listed in the annotated bibliography, Appendix A.

2. Design Considerations

The sensible heat storage system under consideration is shown schematically in Figure 1. It consists of the storage tank and two pumped circulation loops. The water for the source loop is removed from the bottom of the tank, pumped through a heat exchanger (hereafter referred to as the collector) where heat is added and returned to the storage tank at a temperature T_C . The water for the load loop is removed from the top of the tank, pumped through a heat exchanger where heat is removed and returned to the tank at a temperature T_L . Distributors, located within the tank and shown as vertical dashed lines in Figure 1, introduce the return flows at the levels where the return water temperature and the tank water temperature match. When the collector return flow is hotter than any of the stored water and the load return flow is colder than any of the stored water these streams would be introduced at the top and bottom of the tank respectively. For the condition shown in Figure 1 the load return temperature is hotter than the collector return temperature and thus enters the tank at a higher elevation. In an ideal system heat could be stored in the tank and delivered to the load at the same temperature at which it exited the collector. Less than ideal performance will be realized in practice due to:

1. Heat loss to the external environment.
2. Energy degradation due to vertical conduction through the water and tank walls.
3. Energy degradation due to convective mixing.

The absolute and relative importance of these three mechanisms for performance degradation will depend on the application as well as on the details of the tank design. In principle, these effects can be reduced to almost any level desired. Ultimately, economic considerations will set the limit on storage tank performance.

The rate at which heat is lost to the environment in steady state is approximately,

$$q_c = \frac{k_i A_s}{b} (T_s - T_a)$$

Thus, the rate at which heat is lost from a fully charged tank can be easily controlled by varying the thickness, b , of the insulation surrounding the tank. The rate at which the temperature of the stored water drops due to losses or the ratio of heat loss to tank heat storage capacity depends additionally on the tank surface to volume ratio. A spherical tank geometry is optimum from this point of view. For a cylindrical tank the optimum shape is $D/L = 1$. For any tank the ratio of surface to volume decreases with increasing size and external heat losses become less important, for a given storage duration.

Vertical conduction of heat through the water and the tank walls will reduce the availability of the stored energy and tend to reduce the performance

advantage of stratified over mixed storage. The deleterious effects of vertical conduction can be minimized by utilizing a tall cylindrical storage tank with the axis vertical. External heat loss considerations and space limitations generally restrict the utility of this approach. However, the tank can be made effectively taller and side walls conduction effects reduced through the use of internal insulation. Alternatively, the single large storage tank could be divided into a series of small, isolated tanks and conduction losses effectively eliminated. For many applications and in particular for the storage of water at atmospheric pressure for a diurnal charge-discharge cycle such special efforts to reduce vertical conduction are unnecessary.

Convective motions within the tank may be induced by top heat losses, sidewall losses or gains and by vertical conduction through the sidewalls. In a stratified tank these motions may be confined in horizontal cells whose vertical extent will depend on the details of the tank temperature profile. Top losses will tend to create a mixed layer in the upper portion of the tank. The depth of the mixed layer will be determined by the balance between the top losses and vertical conduction. Sidewall losses will locally cool the water near the periphery of the tank resulting in plunging boundary layers. The depth to which these boundary layers fall before leaving the sidewalls and penetrating the interior of the tank will depend on the tank temperature profile. An initially well-mixed tank of hot water will tend to become stratified due to the accumulation at the bottom of the tank of water cooled by sidewall and bottom heat losses. Convection due to top losses and vertical diffusion will act to prevent stratification.

The degree to which stratification can be achieved and maintained in a tank designed for a diurnal cycle will most strongly depend on the way in which the collector and load return flows are introduced into the tank. In order to obtain maximum stratification an inlet must be designed to introduce the flow into the tank at the level where the temperatures of incoming and tank fluids match and to prevent mixing of fluids of unlike temperatures. There is little information available in the literature to aid in the design of an inlet manifold for a stratified storage tank. Consequently, a substantial part of the effort on this project was directed toward the design of a passive inlet distribution system for a stratified tank. The design considerations are described in the next chapter.

An analytical model of a stratified storage tank was constructed to serve as a standard against which the performance of actual storage tanks could be compared. This one-dimensional model is based on the assumptions of complete horizontal mixing and no vertical mixing, except for that required to prevent a destabilizing density gradient due to top losses to the environment. Vertical conduction through the water and tank walls and external heat losses are included. However, mixing of inlet and tank water is neglected. In this sense it is a model of an ideal, stratified tank. Details of this model and the formulation for solution on a digital computer are presented in Appendix B.

3. Inlet Distributors

The essential component of a DIRECT PASSIVE system capable of maintaining stratification under VARIABLE conditions is an inlet diffuser which will remove the momentum of the incoming fluid and minimize mixing while allowing buoyancy forces to position the water at the appropriate level within the tank. Although no references have been found in the literature to previous work dealing with this problem two possible approaches to the design of an inlet diffuser have been identified. One employs a fixed, vertical, porous manifold. The incoming fluid horizontal momentum is reacted by a solid wall, inertial forces are minimized by maintaining a low velocity within the manifold and mixing is inhibited by the enclosing porous walls. Another approach employs a lightweight, flexible hose with one end attached to the inlet and the other free to move vertically within the tank in response to the buoyancy forces due to the density difference between the incoming fluid and the surrounding fluid. Mixing is completely prevented until the incoming fluid discharges from the end of the hose at which point the fluid temperatures are well matched. Both of these approaches can be viewed as attempts to produce a confined, controlled thermal plume. The latter has the advantage of, in principle, completely preventing mixing between fluids of unlike temperature while the former is potentially more reliable since it is immobile and self-purging of entrapped air. Model tests, performed during the early stages of this project, showed that even small amounts of entrapped air would seriously degrade the performance of a flexible hose distributor. Although in many applications the storage fluid would, over a period of time, become gas-free in others, for example service hot water heating, it might not. Consequently, it was decided to concentrate the development effort on the rigid, porous manifold.

This scheme for enhancing stratification in a storage tank under conditions of variable inlet water temperature involves the use of a porous, rigid, vertical distribution manifold. The fluid enters the tank horizontally into a T-section of pipe. The horizontal momentum is reacted by the solid vertical walls of this T-section or reaction chamber. Perforated pipes are connected to the vertical arms of the T-section to form a continuous vertical manifold throughout the depth of the tank. If the incoming fluid density differs from the local tank density at the entry point vertical momentum is imparted to this supply fluid. Under ideal (design point) conditions, which depend on the supply fluid temperature and flow rate and the tank temperature profile, the supply fluid rises or falls in the perforated manifold maintaining a pressure balance with the tank fluid until reaching a level at which the manifold fluid density matches that of the surrounding tank fluid. Under off-design conditions for a given manifold some mixing will occur as the supply fluid moves vertically in the perforated manifold. Either supply fluid will flow out through the perforations or tank fluid will flow into the manifold before the level is reached at which the densities match.

The operation of this inlet has been studied experimentally in scale model tests and documented in a 16 mm motion picture. These tests are described in the following chapter of this report. An analytical model of the inlet operation was developed to provide scaling information. This model is described in the following paragraphs.

As has been suggested earlier, successful introduction of water to the storage tank without excessive mixing requires elimination of the inlet momentum of the new material. In the sketch of the porous inlet, Figure 2, the new fluid is shown as coming in horizontally, perhaps halfway down the height of the storage tank. The horizontal momentum of the new (or "return") fluid is eliminated by the inlet Tee section.

The illustration of Figure 2 depicts one of the two possible operating conditions for stratification, the introduction of cool water into a tank which is already stratified with warm (less dense) water near the top and cool water near the bottom. As is confirmed by the various experiments, the cool inlet water flows down the inside of the perforated manifold until it reaches roughly the level where the fluid densities inside and outside the manifold are equal. Then the excess of internal over external pressure permits outflow through the perforated walls. The alternative condition, with introduction of a warm fluid into a cool tank, is susceptible to a similar description with the exception that the manifold fluid flows upward, and this idea has been confirmed by calculation and experiment. The down-flow condition will be used for exposition of the model.

In operation under the downflow condition, it is necessary for the denser liquid to stand to some height h above the bottom of the Tee in order to impart the vertical momentum the fluid needs to flow down the tube against friction and the pressure drop needed to drive flow out the wall perforations. If the flow conditions and the design are exactly in balance, an unusual circumstance, then the manifold flow will be directly down the tube, with no admixture or outflow through the porous walls, until the level of equal densities is reached, at which level all the manifold flow will be discharged into the tank.

The first question to be raised in a discussion of this type flow has to do with preventing inflow and outflow through the porous walls above the equal-density level. With relatively free communication between manifold and tank, what are the conditions which will permit no flow across the perforated walls? Secondly, recognizing that these conditions are unlikely to be met in practice, one inquires as to the vertical distribution of inflow or outflow across these perforated walls as a function of the design and the imposed conditions of flow. The no-out-flow condition will be studied first.

Flow without entrainment or efflux

If the steady-flow momentum equation is written for an infinitesimally long portion of the fluid inside the manifold, there results the ordinary differential equation

$$\frac{d\rho_m}{dz} + \frac{\tau}{A} - \rho_m g = \frac{\dot{m}_i^2}{\rho_m} \frac{1}{A^3} \frac{dA}{dz} \quad (1)$$

where τ is the retarding friction force per unit length of the manifold. Heat transfer through the walls is ignored; thus the manifold density remains constant at its inlet value ρ_{mi} .

The tank pressure, meanwhile, is influenced only by gravity, since there is no motion. Thus

$$\frac{d\rho_t}{dz} = \rho_t g \quad (2)$$

where in general $\rho_t = \rho_t(z)$. The condition for zero entrainment or outflow is that $p_m = p_t$; that is, there is to be no pressure drop across the wall orifices. If this statement is differentiated with respect to z , then equations (1) and (2) can be combined to give

$$[\rho_{mi} - \rho_t(z)]g = \frac{\tau}{A} - \frac{\dot{m}_i^2}{\rho_{mi}} \frac{1}{A^3} \frac{dA}{dz} \quad (3)$$

This equation shows the options in matching the design to the operating conditions. External conditions generally force the value of the left-hand side. Then with τ going essentially as \dot{m}_i^2 , the possibilities for avoiding entrainment include altering the friction to change the first term or altering the cross-sectional area to change the second term on the right-hand side.

In the experiments done to date, the manifold area has been held constant, so this analysis will use the same condition to the effect that (3) becomes

$$[\rho_{mi} - \rho_t(z)]g = \frac{\tau(z)}{A} \quad (4)$$

for no flow across the walls, and the only option for fitting equation (4) is to alter the apparent wall shear by addition or removal of dissipative devices such as baffles.

It is possible at this point also to calculate the height h to which the cold fluid must rise in the Tee to drive the downflow. Noting that the manifold and tank pressures will be identical at z_1 and z_2 , and ignoring diffusion at level z_1 , one gets from the vertical momentum equation

$$h = z_2 - z_1 = \frac{1}{g} \left(\frac{\dot{m}_i}{\rho_{mi} A} \right)^2 + \frac{1}{\rho_{mi}} \int_{z_1}^{z_2} \rho_t(z) dz \quad (5)$$

This calculation will succeed only if z_1 remains within the Tee. Frictional losses in the T-section have been neglected in this formulation

as have heat transfer effects. If $\rho_t(z) = \rho_t = \text{constant}$ between z_1' and z_2 this reduces to

$$h = \frac{(\dot{m}_i/A)^2}{g \rho_{mi} \Delta \rho} \quad (6)$$

where $\Delta \rho = \rho_{mi} - \rho_t$. This is the height to which the cold fluid in the T-section must rise to impart the vertical momentum for flow through a matched perforated manifold. Equations (4) and (6) also apply for the condition of a warm fluid entering a cold tank if the magnitudes of the density differences are used, $\Delta \rho = |\rho_{mi} - \rho_t|$, and if $h = z_1' - z_1$.

Clearly, for a given $\rho_t(z)$ the appropriate $\tau(z)$ can be designed into the manifold, say by inserting resistance elements, to satisfy eqn. 4. However, since τ will depend on \dot{m} this matching will be possible only for a given \dot{m} , $\rho_t(z)$ and ρ_{mi} . Other, off-design, conditions will result in mixing within or outside of the manifold. Also, under off-design conditions, the h obtained in the T-section will be different than that calculated from eqn. 5 since the pressure in the manifold at the bottom of the T-section will be different than that in the tank. For example, if τ is too small the pressure within the manifold will be lower than that in the tank and net entrainment of the tank fluid will occur. In this case h will be smaller than that calculated from eqn. 5. Also, an inevitable shortcoming of a one-dimensional analysis is that momentum changes due to a developing velocity profile are ignored. The relations derived are, however, in qualitative agreement with observations and should provide a reasonable first estimate for scaling the inlet manifolds.

If the size of the manifold is set, for a particular design point, by using eqn. 5 or 6 and a practical limit on h one finds that wall friction alone is not sufficient to satisfy eqn. 4 and that additional resistance elements must be added to the perforated manifold segments. The devices used in the experiments are doughnut baffles or washers placed at appropriate intervals along the manifold. Application of elementary descriptions of orifice flows allows rewriting of (4) to give

$$\left[\rho_{mi} - \rho_t(z) \right] g = \frac{\dot{m}_i^2 \left[\left(\frac{1}{K} \right)^2 - \frac{2 A_o}{A} \left(1 - \frac{A_o}{A} \right) \right]}{2 \rho_{mi} A_o^2 \Delta z} \quad (7)$$

where K is the orifice discharge coefficient, A_o is the area of the hole in the washer, and Δz is the vertical spacing of washers. The coefficient K , usually thought of as being about 0.6, is itself a function of the area ratio, and the dependence is available from curves for the various types of orifices. If these orifice effects are all lumped together into a single function $F(z)$, so that equation (7) becomes

$$F(z) = \left(\frac{A}{A_o} \right)^2 \left[\left(\frac{1}{K} \right)^2 - \frac{2 A_o}{A} \left(1 - \frac{A_o}{A} \right) \right] = 2 g \Delta z \frac{\rho_{mi}}{(\dot{m}_i/A)^2} \left[\rho_{mi} - \rho_t(z) \right] \quad (8)$$

then a design curve such as Figure 3 gives enough information to size and space the washers. It is to be noted that any change in the mass flow or density difference from the design value upsets the balance of equation (8) and thus creates a nonzero pressure drop across the perforated walls. Then there will be inflow or outflow across the walls.

Flow with entrainment or efflux

Suppose water at constant temperature is flowing down inside a perforated manifold and that the pressure inside the manifold at a given level is less than the tank pressure at the same level. How will the inlet mass flow be distributed vertically among the wall holes?

The increment of increase of mass flow rate in the manifold is the mass flow which comes in one layer of holes, and this quantity is calculable by the orifice equation

$$\Delta \dot{m} = \frac{p_t - p_m}{|p_t - p_m|} A_o C_D \sqrt{2 \rho_m} \sqrt{|p_t - p_m|} \quad (9)$$

This form has the advantage that it applies whether $p_t > p_m$ or not but that it never involves taking the square root of a negative number. The value of the first ratio is ± 1 depending on the direction of the pressure drop. If the sidewall holes are thought of as being continuously distributed vertically, then (9) can be rewritten as

$$\frac{d\dot{m}}{dz} = \frac{dA_o}{dz} C_D \sqrt{2 \rho_m} \frac{p_t - p_m}{\sqrt{|p_t - p_m|}} \quad (10)$$

since by continuity all of the added flow must contribute to the growth of the manifold flow \dot{m} .

The vertical momentum equation for a short length of the manifold, including friction as well as the momentum flow rate change due to the added mass, gives

$$\frac{dp_m}{dz} = \rho_m g - \frac{\tau}{A} - \frac{1}{A} \frac{d}{dz} (\dot{m} V)$$

while in the tank the statical equation is

$$\frac{dp_t}{dz} = \rho_t(z) g$$

The difference of these two equations is

$$\frac{d}{dz} (p_t - p_m) = \frac{\tau}{A} + \frac{1}{A} \frac{d}{dz} (\dot{m} V) - g [\rho_m - \rho_t(z)]$$

and if this is integrated once between z_2 and z there results

$$\Delta p - \Delta p_{z_2} = \frac{f \frac{\rho}{A} \dot{m}^2}{2 \rho_m A^2} (z - z_2) + \frac{1}{A} [(\dot{m} V) - (\dot{m} V)_{z_2}] - g \rho_{mi} \left[1 - \frac{\rho_t}{\rho_{mi}} \right] (z - z_2)$$

in which a friction factor f has been introduced to describe the loss term and a stratified density profile $\rho_t/\rho_{mi} = \text{constant}$ has been assumed. The only term which requires a functional relationship to z to permit integration is the last term, and the step-function stratification implied is a realistic and desirable one.

The momentum terms may be written in terms of mass flow as $\dot{m}_m^2/\rho_m A$, and the entire equation may be made dimensionless through use of the parameters

$$M = \dot{m} / \dot{m}_i \quad \text{for mass flow,}$$

$$\zeta = \frac{z - z_2}{\Delta z} \quad \text{for position,}$$

$$\Delta \pi = \frac{\rho_m A^2}{\dot{m}_i^2} (p_t - p_m) \quad \text{for pressure drop across perforations,}$$

$$P_\rho = \frac{g \Delta z \rho_m A^2}{\dot{m}_i^2} \left[1 - \frac{\rho_t(z)}{\rho_m} \right] \quad \text{for density,}$$

$$P_f = \frac{f \rho \Delta z}{2 A} \quad \text{for friction, and}$$

$$P_o = \frac{A}{\sqrt{2} \frac{dA_o}{dz} C_o \Delta z} \quad \text{for the wall perforations.}$$

The result is

$$\Delta \pi = \Delta \pi_{z_2} + P_f M^2 \zeta + (M^2 - 1) - P_\rho \zeta, \quad (\zeta_2 \leq \zeta \leq \zeta_3) \quad (11)$$

in which it is assumed that $P_o = \text{constant}$ over the range. If P_o is not constant, then the last term merely becomes

$$\int_0^{\zeta} P_o d\zeta$$

With these same definitions equation (10) becomes

$$\frac{dM}{d\zeta} = \frac{1}{P_o} \frac{\Delta\pi}{\sqrt{|\Delta\pi|}} \quad (12)$$

and these two equations (11) and (12) constitute, with an appropriate boundary condition, a first-order ordinary differential equation which can be solved for M vs. ζ . While the two equations could be combined, it is more convenient to keep them separate in view of the need to solve by numerical methods due to the nonlinearity of equation (11).

In finite-difference form, (11) and (12) are

$$(\Delta\pi)_i = (\Delta\pi)_{i=0} + (P_f M_i^2 - P_o)(i \Delta\zeta) + M_i^2 - 1 \quad (13)$$

and

$$M_{i+1} = M_i + \frac{\Delta\zeta}{P_o} \frac{(\Delta\pi)_i}{\sqrt{|\Delta\pi)_i|}} \quad (14)$$

Solution of this system demands a guess of the current $(\Delta\pi)_i = 0$ with a "shooting" solution which seeks a stable result at $\zeta < \zeta_3$. If the initial guess of $(\Delta\pi)_i = 0$ is too large, the solution for M vs. ζ diverges upward, with opposite results for too small a guess. By repeated, increasingly precise guesses of $(\Delta\pi)_i = 0$ it is possible to construct a curve of M and $\Delta\pi$ vs. ζ for given values of the flow parameters. A typical result, in this instance for the limiting case of zero friction, is shown in Figure 4. With the parameter values used, the pressure inside the manifold is always less than that in the tank, and the mass flow in the manifold is seen to increase rapidly due to additions through the wall orifices.

It is important in making these inflow calculations to account for the dilution of the manifold fluid by the inflowing fluid from the tank, whose temperature is of course different. On the assumption of constant specific heats, the First Law gives

$$\frac{d}{dz} (\dot{m} T_m) = T_t \frac{d\dot{m}}{dz} \quad (15)$$

which may be integrated directly to give

$$T_m = \frac{T_{mi} + T_t (M-1)}{M} \quad (16)$$

for the common case of $T_t = \text{constant}$. This diluted temperature is then used with the constitutive information for the working fluid to give the density parameter P_ρ , which now varies with downstream position. The results of M vs. ζ where the dilution is included are very substantially different from those where dilution is ignored, and it is clear that in general the inflow calculations require inclusion of the dilution effect. Of course for the outflow situation the manifold density will remain constant at its inlet value.

Results of this entrainment model so far are encouragingly realistic, but there has not been sufficient time to exploit the model extensively, to gain experience with it, or to test it against the experimental data. These activities are to be reserved for the next investigation.

4. Model Tests

A series of tests, were run in transparent Plexiglas tanks. These tests, combining flow visualization and temperature and flow rate measurements, helped in the formulation of the analytical models described in the previous chapter. They also provided quantitative data to check against the predictions of these models.

Tests were run in a one-foot cubic tank to evaluate the performance of various reaction chambers. In all of these experiments the tank was filled with warm water which was initially well mixed. Cold water was introduced horizontally into the reaction chambers which were positioned near the center of the tank. Water was removed from the bottom of the tank to maintain a constant tank level. The tank vertical temperature profile was monitored by ten equally spaced thermocouples. The temperature profile of the fluid within the reaction chamber was recorded from the output of a thermocouple probe mounted on an automatic traversing mechanism. The flow rate and temperature of the water entering the reaction chamber were also recorded. The tests were terminated when the level of the water in the tank cooled by the incoming flow reached the bottom of the reaction chamber. Thus, during the course of the test the water in the tank adjacent to the reaction chamber was warm and well mixed.

The three different chamber configurations shown in Figure 5 were tested. Two of these were T-section inlets in which a single horizontal jet entered a vertical reaction pipe. In the third configuration the jet entered an annular gap which surrounded a vertical perforated pipe.

Temperature profiles measured in the reaction chamber for several of these tests are shown in Figure 6. The level of the flat portion of the profiles near the top to the chambers corresponds to the temperature of the water in the tank surrounding the chamber. The fact that the temperature near the top of the chamber is constant implies that some tank fluid is being drawn into the top of the chamber, entrained by the incoming water and ejected out the bottom of the chamber. The region of mixing between these two flows corresponds to the region on the profiles where the temperature varies erratically with position. In the mixing region the temperature fluctuates with time and these curves represent one realization of the time dependent profile. The mean temperature profile in the mixing region does remain stationary however.

The top three curves, Figures 6a-c show the effect of flow rate on the location of the abrupt temperature drop within the annular reaction chamber. If the flow rate is increased beyond the level corresponding to Figure 6c cool water will be forced out the top of the reaction chamber. The location of the abrupt change in mean temperature with respect to the bottom of the reaction chamber is compared with the theoretical position of the interface between the hot and cool fluids predicted from the model discussed in the last section in Figure 7. Since the tank temperature and inlet temperature varied from run to run the experimental data were corrected to a standard density difference of 0.3 lbm/ft^3 using equation 6 to permit a graphical presentation of the results. Since in many of the

experiments the mean temperature of the water in the mixing region varied somewhat with position an integrated average was used to characterize the density of the fluid below the interface.

These experiments show that the actual interface location is higher than that predicted by theory for the same density difference. This is because the buoyancy forces must impart vertical momentum not only to the incoming water but also to the water entrained in through the top of the reaction chamber. The results indicate that the entrainment mass flow is smallest for the annular reaction chamber and largest for the T-section with the inlet near the top.

An independent determination of the entrainment flow rate can be obtained from mass and energy balances for the reaction chambers. When the data plotted in Figure 7 is moved to the right by an amount equal to the calculated entrainment flow rate the agreement with theory for the annular reaction chamber is very good as illustrated in Figure 8. The agreement for the other two configurations is less good. The discrepancy may be attributed to incomplete mixing at the exit of the reaction chamber for these two configurations. Thus, if the velocity profile is not uniform the momentum of the fluid leaving will be larger than that for the same mass flow rate and uniform exit velocity. Also, if the temperature of the fluid in the reaction chamber is not uniform then the density, as determined from a single vertical profile, may be in error.

The annular configuration was chosen for all further tests since it appeared to be the most predictable of the three tested and yielded the smallest entrainment. The ratio of the mass flow rate entrained in through the top to the inlet mass flow rate is plotted in Figure 9 as a function of inlet mass flow rate. The entrainment approaches zero as the interface approaches the top of the reaction chamber, $m \approx 50 \text{ lbm/hr}$.

Additional model experiments were run in a two-foot cubic Plexiglas tank. The purpose of these experiments was to obtain qualitative and quantitative information concerning the effect of the perforated section of the inlet manifold on tank stratification. For this purpose a standardized test was used. Common to all tests was an annular reaction chamber similar to that shown in Figure 5 but 4 inches in height and $1\frac{1}{2}$ inches in inside diameter. This reaction chamber was positioned near the upper part of the tank so that its upper opening was $1/2$ inch below the level of the water. Vertical extension tubes, $1\frac{1}{2}$ inch I.D., could be attached to the lower end of the reaction chamber to complete the manifold. The inlet to this manifold was biased toward the top of the tank to favor tank charging. This would be the preferred configuration for a manifold designed to introduce collector-return water into the tank in a system in which the collector outlet temperature was higher than the highest tank temperature under most conditions.

The standardized test, which was run for a number of manifold configurations, consisted of introducing hot water into an initially well-mixed cold tank until it was about half charged. At this point the collector return water, which was removed from the bottom of the tank, was recycled

into the inlet without external heat addition. The flow rate was maintained at 300 lbm/hr throughout the duration of the test. The temperatures of the incoming water and the tank at 20 equally spaced vertical locations were recorded.

The temperature history of the inlet water and tank temperature profiles at several times are shown in Figure 10 for one test. In this test the reaction chamber was used without any perforated extension. The results show that good stratification was achieved during the initial charging period. The solid line shows the theoretical temperature profile at the end of the 45 minute charging period. At the end of this period the inlet temperature drops almost to the temperature of the water at the bottom of the tank as the recycling period begins. The slight excess of inlet temperature over tank bottom temperature is due to the heat added to the fluid as it passed through the top layer of the tank to reach the reaction chamber. Dye added to the incoming water shortly after the change in inlet temperature, $t = 50$ min, revealed that all of the locally cool incoming water was emerging from the bottom of the reaction chamber in a turbulent jet which spread into a horizontal band extending from a height of about 7 in. to 12 in. The test was terminated at $t = 120$ min. at which time the difference between the temperatures at the bottom and top of the storage tank had been reduced to about 18°F . In absence of mixing, and neglecting the slight heating of the incoming water, the tank temperature profile at this time would have been little changed from that existing at $t = 45$ min. Diffusion and heat loss to the environment would have only a small effect over this time period.

Although the reaction chamber alone was effective in promoting stratification during the charging period the tank became almost completely mixed below the level of the reaction chamber by the end of the test. In an attempt to reduce this mixing a perforated extension tube was added to the bottom of the reaction chamber. This $1\frac{1}{2}$ inch I.D. Plexiglas tube extended down to within one inch of the bottom of the tank. It was open on the bottom and perforated along the sides with $1/4$ inch holes. The measured temperature profiles for this test, Figure 11, indicate only a slight improvement in the stratification preserved during the recycle period as compared to the reaction chamber alone. Visualization during the recycle period indicated entrainment in through the top of the reaction chamber and through the perforations just below the reaction chamber. All of the water flowing down through the tube was expelled out the perforations and none through the bottom of the tube. The dyed water formed a band within the tank extending from about 4 in. to 11 in. In order to assess the effect on overall tank mixing of the fluid entrained in through the top of the reaction chamber this test was repeated with one change. At the beginning of the recycle period, $t = 45$ min., the top of the reaction chamber was sealed. The temperature profiles for this test, Figure 12, show that this tended to isolate the layer of hot water in the tank located above the lower end of the reaction chamber from the mixing which continued unabated in the lower part of the tank.

In the final test to be described here resistance elements were added to the perforated tube in an attempt to match the pressure within the

manifold to that in the tank in the upper section of the tube to reduce the entrainment of hot tank water in through the perforations. The resistance elements consisted of 10 steel washers supported at equally spaced vertical locations by crossed wires laced through the perforations. These washers were sized by the method described in Chapter 4 to match the pressure drop with a uniform, 30°F temperature differential between the manifold and tank fluids. The results of this experiment are shown in Figure 13. The degradation of the stratification during the recycle period is noticeably reduced compared to the other configurations tested although the performance is still far from ideal. Visualization revealed a small outflow of manifold fluid at the top of the tube where, in absence of resistance elements, there was entrainment. Clearly, the concepts presented in Chapter 3 are correct. Additional tuning experiments are required to determine how closely the ideal performance can be approached in practice.

5. Prototype Tests

A prototype storage tank was constructed and tested to simulate operation in an actual solar installation. The tank volume, flow rate and heating rate correspond roughly to a system with 300 ft² of collector surface with storage sized for the diurnal cycle.

The prototype tank is a steel cylinder having 3/16" wall thickness, inside diameter of 45-5/8" and inside height of 84". The tank is filled with water to the 80" level thus the storage volume is 75.69 ft³ or about 566 gallons.

The tank walls are wrapped with one layer of kraft paper backed R-11 fiberglass insulation. The top is covered with 6" thick styrofoam rated at approximately R-27. The bottom of the tank, which is supported 8" from the floor, is uninsulated due to the potential moisture problems involved, except for a skirt of R-11 fiberglass around the circumference of the tank, which is continuous from the tank walls to the floor.

Temperature profiles in the tank are monitored by thermocouples spaced 8" from the tank wall, midway between the collector and load return manifolds, and at 4" vertical intervals starting 2" from the bottom of the tank. The thermocouples are held in place by a 1/2" PVC pipe from which the thermocouples project 1 1/2". The inlet manifolds were designed on the basis of the information presented in the last two chapters. A reaction chamber height of 6 inches was selected as a reasonable compromise in the trade-off between height and diameter. Equation 6, plotted in Figure 14, indicates that for a 30°F difference in temperature between the tank and inlet flow a reaction chamber diameter of 3 inches would be sufficient to prevent overflowing the reaction chamber at the design flow rate of 3000 lbm/hr. A four inch diameter was selected to allow for operation under smaller temperature differences and to accommodate a change in the design of the annular inlet. In the prototype manifold the water enters through the central one of two concentric pipes and flows radially outward into the annular reaction chamber. This design was adopted to simplify the plumbing and installation. The location of the reaction chambers were biased, collector chamber up and load chamber down, to favor operation under FIXED conditions. The collector water, thus, enters the annular manifold near the top of the tank and either flows up and out into the tank if it is hotter than the surrounding fluid or down the annular duct and out through the perforations. The porosity of the perforated outer shell in the prototype was matched with that of the manifold used in the model tests. The diameter of the perforations was made much larger in the prototype however to simplify construction. Ideally, the holes should be small to minimize shear induced mixing. This, of course, is the principal function of the manifold. A further discussion of this point is contained in the final chapter of this report.

The similar 76" long collector and load return manifolds are constructed of 4" nominal PVC drain pipe, 22 horizontal rows of 1" holes, 4 holes, spaced radially 90° apart, per row, are drilled at 3" vertical intervals starting 6" from the top of the collector return manifold

(6" from the bottom of the load return manifold). The axes of the holes in each row are staggered 45° from the axes of the holes in adjacent rows.

A 1" nominal PVC pipe is positioned concentrically inside each 4" pipe. The 1" pipe is capped at the bottom. Seven rows of 3/16" holes, in configuration similar to the 4" pipe, are drilled at 1/2" vertical intervals starting 1 1/2" from the top of the collector return manifold (1 1/2" from the bottom of the load return manifold). Water returning from the collector flows through the 1" pipe which enters the tank at the top and out the 3/16" holes near the top of the manifold where it rises or falls within the manifold to the proper level according to its density and then flows horizontally out the 1" holes (or out the top or bottom of the manifold). Water flow in the load return manifold is similar except that it must travel the full length of the manifold within the 1" pipe before flowing out the 3/16" holes near the bottom of the manifold.

The manifolds are diametrically opposed 16" from the tank walls and 2" from the bottom of the tank.

A schematic diagram of the prototype system is shown in Figure 15. Collector water exits the tank through a 1 1/4" PVC tee placed in the center of the bottom of the tank. The ends of the tee face 90° from the manifolds 2" above the bottom of the tank. Water flows into either end of the tee and out the bottom of the tank into the collector loop pump. From the pump the water flows through a gas fired water heater into a 275 gallon "capacitor" tank which damps oscillations in the water heater outlet temperature. From the tank the water flows through a temperature controlled mixing valve and an orifice for measuring the flowrate and then returns to the storage tank via the collector return manifold.

Piping is provided to bypass a) the capacitor tank, and b) both the water heater and the capacitor tank. Bypass b) provides cold water to the mixing valve. Bypass a) allows the storage tank to be heated without effecting the temperature of the capacitor tank.

Load water is extracted from the tank through a 1" PVC tee immersed 2" below the surface of the water in the center of the tank in a position similar to that of the collector loop tee. From the tee the water travels through a pump and the shell side of a shell and tube heat exchanger where it is cooled by tap water circulating through the tube side. After traveling through an orifice for flowrate measurement the water then returns to the storage tank via the load return manifold.

Twenty tank segment temperatures, collector return temperature, load return temperature, collector exit temperature, load exit temperature capacitor tank temperature and room temperature are all measured using copper-constantan thermocouple junctions and recorded by a Doric Digitrend 220.

Collector flowrate and load flowrate are monitored by measuring the pressure drop across an orifice. Validyne model DP15TL pressure transducers transmit the signals through Validyne model CD15 carrier demodulators to the Doric recorder.

Water from the collector exit flows through an Oberdorfer model 700C USM pump and an Ack-o-matic model 21W4S gas fired water heater controlled by a United Electric type 600 model 6BS temperature controller.

Hot water from the capacitor tank and cold water from the water heater bypass is mixed in a Power model 1 P1 mixing valve regulated by a Power Accritem model 3 P3 temperature control.

Load exit water flows through a Burkes model SCTSM pump and a Young Radiator model F-303-HY-4P heat exchanger.

A preliminary test was run to determine the actual heat losses from the tank to the environment. In this test a stratified temperature profile was established in the tank by running the collector and load loops for some period of time. Once the desired stratification was obtained the flows were stopped and the tank was allowed to react to external losses and vertical diffusion. The loss coefficients in the ideal computer model were then adjusted so that the predicted and measured profiles agreed. The final comparison between the data and the predictions are shown in Figure 16.

Six additional tests were run to simulate operation in a solar system. These include: 1) charging, 2) charging at low flow rate, 3) discharging, 4) partial charging with recycling, 5) partial discharging with recycling, and 6) simultaneous charging and discharging. The measured tank temperature profiles for each test are plotted in Figures 17 through 22 and compared with the predictions of the ideal, non-mixing tank.

The two charging tests gave similar results. In the high flow rate charging test (Fig. 17) note that the theoretical analysis maintains several inches at the top of the tank near 105 degrees but the test data does not show this. During the test the collector return temperature dropped gradually from 107° to 99° at 1.5 hours while the flow rate remained constant at 3000 lb/hr. The test data show that upper portion of the tank is mixed and that the mixed portion in each case is somewhat greater than the portion in the theoretical analysis which is near uniform temperature. The experimental thermocline is sharper than the theoretical thermocline, which would also indicate mixing down to the level at which the thermocline begins.

The low flow rate charging experiment (Fig. 18) at 1750 lb/hr also shows greater mixing than theoretical but the transition from the mixed portion and the thermocline is not as sharp as in the high flow rate experiment.

The discharging experiment (Fig. 19), at a flow rate of 2020 lb/hr, looks, as expected, like an upside down charging curve, with slightly greater mixing and sharper thermoclines than theoretical.

In the partial charge-recycle experiment the heated collector flow was run until the initially well-mixed, cool tank was approximately half charged at which time the collector heat input was dropped to zero but the flow

maintained. The results, shown in Figure 20 for a flow rate of 3100 lbm/hr indicate that relatively rapid mixing took place in the bottom half of the tank following the change to recycle conditions at 0.8 hrs. The performance of the prototype tank under this severe test is similar to that of the 2 ft. tank with a perforated manifold having no resistance elements. The results of the discharge-recycle experiment, Figure 21, are comparable. Note that the theoretical ideal temperature profiles for the last two experiments remain virtually unchanged during the recycle periods.

In the final experiment an initially nearly uniform tank was subjected to simultaneous charge and discharge flows. The collector and load flow rates were maintained nearly equal at 2000 lbm/hr and 2020 lbm/hr respectively. The tank temperature profiles, Figure 22, show nearly ideal performance with evidence of only slight mixing at the upper and lower thermoclines. Another indication of the performance under these conditions is the match between inlet and outlet temperatures. The temperature histories shown in Figure 23 illustrate the small loss in availability of energy in the stratified tank. The temperature of the water delivered to the load is only about 1°F lower than that supplied by the collector. Similarly, the water delivered to the collector is about 1°F warmer than the makeup water supplied to the tank.

In general, the results of these prototype tests mirror those obtained in the model tests. Stratification was easily achieved and maintained for FIXED inlet conditions. Performance under the severe VARIABLE inlet condition test run was poor compared to the theoretical, non-mixing, ideal tank. A substantial performance improvement could be anticipated, however, through the judicious use of resistance elements in the prototype manifold. The theory developed in Chapter 3 should prove a valuable aid in selecting the proper elements.

6. The Effects of Stratification on System Performance

The study of Duffie and Beckman referred to in the Introduction indicated that a significant increase in performance could be realized in a solar water heating application if the storage tank could be stratified. The study, described in this chapter, was made to see if a similar increase would be realized in a space heating application. The approach used was similar to that of Duffie and Beckman. The operation of the system was simulated over a certain period of time using a computer model and the predicted fraction of the total heating load carried by solar determined. Each simulation was run twice, one with a mixed storage tank model and once with an ideal stratified tank model and the load fractions compared.

There are a number of system parameters which must be set before a simulation can be made and each of these may influence the relative advantage of a stratified storage tank. A major portion of this study was devoted to an assessment of influence of these parameters. In order to accomplish this without an excessive expenditure of computer time a simplified space heating system model was used.

System Description

The simplified system configuration shown in Fig. 24 was chosen to minimize computer time yet produce a reasonable representation of a solar heating system with which parameter sensitivity could be studied.

Weather Data: Seven days of hourly weather data for January in Boulder, Co. from Table 3.3.3, Duffie and Beckman, was used (see Fig. 25). The data was not interpolated except for model validation using TRNSYS. Collector slope was set at 40 degrees, thus providing the same insolation on the tilted surface for each simulation.

Collector: The collector is modelled by the equation

$$q_u = A_c F_R [H_T (\tau\alpha) - U_L (T_w - T_a)]$$

where

$$F_R = \frac{\dot{m}_c c_p}{U_L A_c} \left[1 - \exp(-U_L A_c F' / \dot{m}_c c_p) \right], \quad F' = U_o / U_L$$

The collector loss coefficient is assumed not to change with wind speed or absorber plate temperature. Heat capacity effects are neglected.

Collector Loop Pump and Controller: The collector pump is turned on whenever q_u becomes positive. The simulated controller provides no hysteresis. The flow rate through the collector supplied by the pump is constant, except in control mode 3.

Pressure Relief Valve: The collector outlet water flows directly into the tank without losses through the piping and without passing through a

heat exchanger when the outlet temperature is below the boiling point of water. When the collector outlet temperature is above the boiling point the temperature it is reset to 100 C, thus simulating the operation of a pressure relief valve. Loss of mass through the valve is considered negligible.

Thermal Storage Tank: The storage tank provides optimal thermal stratification and is described in Appendix B.

Losses from the tank are assumed not to contribute to supplying the load. Tank losses are, however, assumed to be to room temperature.

Load: The load is modelled by the equation

$$\frac{q}{T_L} = (UA)_L (T_r - T_a)$$

where UA is a specified constant.

The load is supplied via a heat exchanger which is modelled using a constant effectiveness analysis. The equations are

$$\begin{aligned} q &= \dot{m}_L c_{pL} (T_i - T_L) = \dot{m}_r c_{pr} (T_{ro} - T_{ri}) \\ &= e C_{min} (T_i - T_{ri}) \end{aligned}$$

where C_{min} is assumed to be $\dot{m}_r c_{pr}$, which is the usual case in a water to air heat exchanger.

The criteria for supplying the load from thermal storage and/or from auxiliary and the method of modulation of the mass flow rates and temperatures is determined by the system control modes.

System Control Modes

Mode 1: In mode 1 a load side outlet fluid minimum temperature is specified. From this minimum temperature and the load heat exchanger data a minimum reference tank temperature is calculated. For a space heating system utilizing forced air the fluid would be air and the load side outlet fluid minimum temperature would be about 40 C for human comfort. For a room temperature of 20 C and a perfectly efficient load heat exchanger the reference tank temperature would be 40 C.

As long as the minimum outlet temperature can be obtained by heating from storage then the storage-load pump stays on whether the quantity of energy available from storage is sufficient to supply the entire load or not. When the top tank segment temperature drops below the reference tank temperature the storage-load pump is turned off.

When storage can potentially provide more energy at an acceptable temperature than is needed to supply the load, the storage-load pump need operate for only part of the time step to meet the load requirement. To simulate operation of the pump for only part of the time step, the mass flow rate through the loop is reduced while the outlet temperatures corresponding to the maximum mass flow rate are retained.

Mode 2: In mode 2 the storage-load pump is on until the top tank segment temperature drops below a reference temperature specified by the user. If the reference temperature were set equal to the room temperature, then the storage-load pump would be on virtually all the time, thus, during long periods of low solar insolation, draining nearly all the available energy from the storage tank. If the reference temperature were 75 C the system would operate much like an absorption cooling system, in which high temperatures are required for the operation of the cooling cycle.

When storage may provide more energy than is required by the load the storage-load loop mass flow rate is modulated as in mode 1.

Mode 3: In mode 3 the collector mass flow rate is modulated such that the collector outlet temperature is greater than the reference tank temperature described in mode 1 whenever the top tank segment temperature is less than the reference tank temperature. When the top tank segment temperature is equal to or greater than the reference tank temperature or when the collector outlet temperature at the maximum mass flow rate is greater than the reference tank temperature, then the collector mass flow rate is set to the maximum.

Load side control in mode 3 is the same as in mode 1.

Mode 4: Mode 4 is provided for comparison to the TRNSYS load model. Instead of modulating the mass flow rate through the storage-load loop at constant outlet temperature conditions during a time step to achieve energy balance, the simple TRNSYS model and mode 4 modulate the heat exchanger outlet temperatures at constant mass flow rate conditions.

Results

A base system was chosen to reflect a typical water space heating system and load requirement. Input parameters, in SI units, were as specified in Table 1. Many computer runs were made, in each case varying one parameter.

Number of Tank Segments, Time step: Initially a number of tank segments were chosen by comparing the results of several computer runs using different numbers of tank segments. In each case a time step was used which was calculated to be the maximum allowable for thermal stability. As seen in Fig. 26, where the fraction of the total load carried by solar f is plotted versus number of segments and/or time step, 20 tank segments yielded the greatest advantage due to stratification while providing acceptable accuracy and computer time requirements.

It should be noted that for a constant time step f_{strat} increases as the number of tank segments increases. The fact that Fig. 26 shows a decrease in f_{strat} as the number of tank segments increases above 10 reflects the magnified integration error of the digital computer caused by the increased number of computations due to the decreased time step.

Collector Mass Flow Rate: Fig. 27 shows an increase in the advantage due to stratification as the collector mass flow rate is decreased. Note that with a stratified tank an optimum flow rate exists where the load fraction is greatest. With a mixed tank the load fraction increases monotonically with flow rate. A much lower flow rate and correspondingly lower pumping costs are possible using stratified storage in a system yielding performance equivalent to the same system using mixed storage.

Collector Loss Coefficient: Fig. 28 shows a decrease in the load fraction supplied by both stratified and mixed systems as the loss coefficient increases, the advantage due to stratification also increases, however, it does not do so monotonically. There is a peak at $U_L = 15$ and a low at $U_L = 18$. This behavior is unexpected and unexplained at this time.

Building Loss Coefficient: As the load requirement increases the load fraction supplied by both stratified and mixed systems decreases as shown in Fig. 29. This would be analogous to reducing the collector area for constant load requirement. Note that the advantage due to stratification is relatively insensitive to this parameter.

Reference Tank Temperature: As might be expected, the minimum temperature at which stored energy can be used greatly effects the advantage due to stratification as shown in Fig. 30. When the reference tank temperature is equal to the room temperature the advantage due to stratification is about one percent, but when the reference temperature is raised to 75 C the advantage is over 15 percent. Thus, stratification holds great promise in increasing the performance of systems which must supply energy at high temperatures, such as absorption cooling systems.

Tank Volume: Storage must be provided in solar heating systems to supply energy to the load during times when energy is not available directly from the sun. The storage volume may be sized for a series of cloudy days, it may be sized to supply the load during the night, or it may be sized for an annual cycle in which energy is stored during the summer for use in the winter. The longer the energy storage cycle the larger the storage capacity must be. The point must be made that in a simulation of short duration, the choice of the initial tank temperature is critical to the usefulness of the resulting performance data. If, for instance, a low initial temperature were chosen for a large tank, the system might require several days to raise storage to a useful temperature. The larger the storage volume the greater the potential error will be.

The initial tank temperature in each simulation was 50 C. In the base system the storage volume was sufficient to heat the load from the beginning of the simulation at 12:00 midnight until the sun came up the first day at

about 8:00. Larger volumes would supply the load for a longer time. The largest tank simulated was three times larger than the base system tank. It could be expected to supply the load for roughly 24 hours, 16 hours longer than the base system tank. It is assumed that during the 168 hour simulation the potential error resulting from a greater initial quantity of stored energy is diluted to the point that the results are still useful for comparison.

This potential error could be reduced if, by trial and error, the tank temperature at the end of the simulation could be matched to the initial tank temperature.

Fig. 31 shows that the advantage due to stratification increases as the tank volume increases. A larger storage volume not only allows the storage of greater quantities of energy, but also reduces the average collector inlet temperature, thereby increasing collector performance.

Tank Height/Diameter Ratio: The tank height/ diameter ratio might be expected to increase the advantage due to stratification, but, as shown in Fig. 32, the effect is minimal in a system which maintains optimum stratification. The effect may be greater in a system which allows for some mixing of the collector and load inlet water with surrounding tank segments as the water enters the prescribed segments.

If optimum stratification can be achieved in a tank of any height/diameter ratio, then Fig. 32 shows that for maximum system performance the height/diameter ratio should not exceed one, which is the shape yielding the minimum surface/volume ratio.

Other System Parameters: The tank loss coefficient was found to have little effect on the advantage due to stratification.

Reducing the effectiveness of the loadside heat exchanger reduced the load fraction carried by both stratified and mixed systems and increased the advantage due to stratification slightly.

Increasing the desired room temperature has the effect of increasing the load requirement. It also effects the losses from the tank. As the desired room temperature increases, the load fractions and the advantage due to stratification both decrease.

For the tank and system simulated, conduction from one segment to another along the tank walls had an insignificant effect on the load fractions and the advantage due to stratification.

Neglecting conduction through the water resulted in a less than .1% change in the load fractions. These factors could be expected to be more important in a system where larger temperature differences in the tank are involved, such as in service hot water systems where make up water temperature may be less than 10 C.

Mode 3, in which an attempt is made to control the collector mass flow rate such that the collector outlet temperature is always above a minimum useful temperature, showed very little advantage over mode 1, in which the collector mass flow rate is not controlled. Collector mass flow rate control may be more advantageous in a system in which the collector outlet water may pass directly to the load heat exchanger, bypassing the storage tank, where the several losses involved may degrade the temperature and the usefulness of the collector outlet water.

Model Validation

In order to check the validity of the simplified system model, a similar TRNSYS model using a fully mixed tank was developed. The information flow diagram for the TRNSYS model is shown in Fig. 33.

A number of peculiarities in the TRNSYS system components made it necessary to modify the simplified model to obtain a good comparison. TRNSYS interpolates weather data so interpolation was added to the simplified model. Control mode 4 was used in the simplified model to provide comparison the TRNSYS load mode 2.

The difference in the methods of intergration between the two models caused a substantial difference in the results. Using the base system parameters in each case, the simplified mixed tank simulation resulted in a total load of $3.92 \times 10^6 \text{ KJ}$ of which 70.49% was carried by solar while the TRNSYS simulation resulted in a load of $4.39 \times 10^6 \text{ KJ}$ of which 62.58% was carried by solar.

Since the loads in both simulations are calculated using the same equation and the same variables, the difference in the results must lie in the method of integration. Adjusting the building loss coefficient in the TRNSYS simulation so that the total load becomes equal to the total load in the simplified simulation, the load fraction becomes 68.27%, a 3.15% difference in the two answers.

Discussion

The results show that an improvement in system performance is possible with stratification in all cases; however, the magnitude of the improvement depends upon several key parameters.

The system presented benefitted most from stratification when the model included low collector mass flow rates, low load requirements relative to the collector area, large tank volumes or high temperatures required of the load. Caution should be used, however, in extrapolation of the results presented to other systems. For example, a simulation using a building load of 200 KJ/hr C, a collector mass flow rate of 1500 Kg/hr, a reference tank temperature of 75 C (control mode 2) and all other system parameters the same as the base system resulted in an advantage due to stratification of 12.48%. Increasing the tank volume to 12 m³ decreased the advantage to 9.39%. It is obvious that each proposed solar heating system will react differently to changes in the system parameters. A study of the key parameters, which have been identified, should be made in each case to determine the most efficient system design.

7. Conclusions

The results of this study indicate that nearly ideal stratification can be attained in storage tanks in solar applications in which the inlet conditions are FIXED. One such application would be for service hot water heating with collector flow rate controlled to maintain its exit temperature at least as high as the hottest storage water. The only special feature required to achieve and maintain stratification is an inlet which minimizes mixing. The cost of such an inlet is negligible and if installed at the time of system construction it would not measurably change the total system cost.

A simple passive inlet for applications in which the inlet conditions are VARIABLE has been proposed. Theory and experiments show that this inlet will reduce mixing and promote stratification even under conditions in which the water entering the tank is at a temperature between the storage temperature extremes. Although, even in theory, this rigid porous inlet manifold cannot be designed to completely prevent mixing over a range of inlet conditions it can be used to minimize the deleterious effects on stratification of off-design inlet temperature excursions in an almost FIXED system.

Theory has revealed the possibility for a significant improvement in the design of an inlet for VARIABLE conditions. This would involve replacing the rigid, porous wall of the vertical manifold with a flexible, porous wall. This manifold would tend to minimize the pressure differentials which force unwanted entrainment or efflux by changing its cross-section. If this manifold were constrained to a vertical orientation any air bubbles introduced with the incoming flow would be free to rise to the top of the tank without interfering with its operation.

Finally, a study of the effect of stratification on the performance of a solar heating system showed that, depending on the system design, stratification can provide a 5 to 10% increase in the heating capability of a solar system.

APPENDIX A

Annotated Bibliography

Experiments

1. Close, D. J., "The Performance of Solar Water Heaters with Natural Circulation," Solar Energy, 6, 1, p. 33, 1962.

Measurements show stratification in a water storage tank in a natural circulation system. No details on the internal construction of the 30 gal., 16 in. dia x 41 in. high tank are given. Comparison between the performance predicted assuming perfect stratification in the tank and measured performance during charging on a sunny day with no load is good.

2. Davis, E. S. and Bartera, R., "Stratification in Solar Water Heater Storage Tanks," Proc. Workshop on Solar Energy Storage Subsystems for the Heating and Cooling of Buildings, Charlottesville, Virginia, April 1975, p. 38, ASHRAE, 1975.

Experiments on a tank containing 450 gallons of water indicated stratification under certain operating conditions. Data are presented which show that stratification can be maintained throughout a night demand cycle starting with an almost uniform 135°F tank and adding 60°F makeup water at the tank bottom. When warm water from the collector was introduced into the tank at midheight near the end of the discharge period mixing with the cold makeup water apparently took place. In another test, with makeup water at intermediate temperatures introduced at tank midheight, much less stratification was observed. No comparisons are made with the theoretically maximum (no mixing) stratification possible under the conditions of these tests.

3. Phillips, W. F. and Cook, R. D., "Natural Circulation from a Flat Plate Collector to a Hot Liquid Storage Tank," ASME paper 75-HT-53, AICHE-ASME Heat Transfer Confr., August 1975.

A small scale solar system with a water storage tank (0.19 m² collector and 0.01 m³ tank) was tested and the results compared with an analytical model. The authors claim that the data indicate performance somewhere between well-mixed and perfectly stratified conditions in the storage tank. Few details of the experiment are presented.

4. Cooper, P. I., Klein, S. A. and Dixon, C. W. S., "Experimental and Simulated Performance of a Closed Loop Solar Water Heating System," abstract of presentation at the ISES meeting Rockville, MD., 1975.

A pumped circulation system with liquid storage was tested. Few details are presented in this abstract, however, the following paragraph indicates that some stratification was achieved.

PRECEDING PAGE BLANK

"Initial experimentation indicated that the stratified storage tank model of Close[2] was possibly not sufficient for comparison of experimental and simulated performance on an instantaneous basis. Examination of the measured storage tank temperatures suggested that a more representative 'black-box' model of the tank could be devised and used in TRNSYS. This model was found to more closely approximate the short-term performance of the storage tank, though it is suspected that a simple, unstratified model will be sufficient for long-term performance predictions."

Note: Their ref. [2] is our ref. [7].

5. Lavan, Z. and Thompson, J., "Experimental Study of Thermally Stratified Hot Water Storage Tanks," Submitted for publication in Solar Energy Journal, 1976.

A systematic study was made on the effects of geometry, flow rate and temperature difference on stratification in scale model water tanks. The operating conditions were the same as those found by Davis and Bartera [2] to promote good stratification; an initially well-mixed tank of hot water with withdrawal at the top and cold makeup water introduced at the bottom. An inlet manifold designed to minimize mixing is described.

6. Solar Total Energy Program Semiannual Report, R. W. Harrigon, ed., October 1974 - March 1975, SAND 75-0278, Sandia Laboratories, 1975.

A 2000 gal. tank designed to store Therminol 66 at 600°F is briefly described. Additional information obtained from personal communication with J. A. Leonard of Sandia indicate that stratification is achieved during charging and discharging. During charging the incoming fluid is maintained at 590°F and introduced at the top of the tank through a diffuser. During discharge cool, 470°F, fluid is introduced at the bottom of the tank. The system operates so as to maintain the inlet temperatures at the storage extremes.

Theoretical

7. Close, D. J., "A Design Approach for Solar Processes," Solar Energy, 11, 2, p. 112, 1967.

Close describes the precursor of a model for a stratified storage tank promulgated by Duffie and Beckman [9]. The model, as employed by Close, has two deficiencies: a) vertical conduction through the liquid is ignored and b) vertical mixing occurs when both collector and load flow rates are non-zero. The omission of vertical conduction could be important for small tanks and has the effect of overpredicting stratification. The vertical mixing, which is a maximum in the model when the flow from the collector is hotter than the liquid at the top of the tank and the flow from the load is cooler than the liquid at the bottom of the tank (just the reverse of the actual physics), tends

to degrade the stratification and thus yield results which underestimate the efficacy of stratified storage.

Based on this model for storage and a single system simulation with both three and six segment approximations for a stratified tank Close concludes that a three segment approximation is adequate for system performance prediction. Apparently no one has since used more than three segments to model a stratified tank.

8. Brumleve, T. D., "Sensible Heat Storage in Liquids," Sandia Laboratories Energy Report SLL-73-0263, 1974.

An analysis is carried out of several problems associated with stratified storage including: heat loss to the environment, conduction at a thermocline and mixing. This report summarizes preliminary design work done prior to the construction of the 2000 gal. tank described in [6].

Economics

9. Duffie, J. A. and Beckman, W. A., Solar Energy Thermal Processes, Wiley, p. 247, 1974.

A single simulation comparing mixed vs. stratified storage for a water heating application shows a 6% increase in the percentage of the load carried by solar energy when storage is stratified. A three segment model, apparently the same as Close's, was used.

APPENDIX B.

IDEAL STRATIFIED TANK MODEL

The fluid storage tank is divided into a number, N , of isothermal constant volume segments of height Δz . Since the variation of thermal conductivity and density of water over the range of temperatures of interest in solar space heating and cooling applications is small, these quantities are taken as constant. Thus, for a constant cross-section tank, all segments are of equal mass and shape. Other storage fluids can be modeled by making the appropriate changes in fluid properties.

Fluid from the collector enters the hottest segment whose temperature is less than or equal to the collector return temperature. Fluid from the load enters the hottest segment whose temperature is less than or equal to the load return temperature. Collector fluid is always drawn from the bottom of the tank and load fluid from the top.

The model is designed to give results for the ideal case in which no mixing occurs except that which occurs due to negative temperature gradients. Negative temperature gradients occur when an upper segment has a lower temperature than the segment below it. This situation may often exist since the top tank segment has a greater surface area exposed to the environment than do middle segments.

Each segment is subject to certain thermal losses. (See Figure B1.) Losses to the environment from each segment can be computed using an overall loss coefficient for each segment, the segment temperature and the ambient temperature of the tank environment.

$$q_{ei} = (UA_s)_i (T_i - T_a)$$

Losses from each segment to the segments above and below it can be computed using the conductivity of the fluid, the tank cross-sectional area, the distance between segment centers and the segment temperatures. Conduction along tank walls may also be significant. Assuming that the fluid and the adjacent walls are the same temperature, an overall conduction coefficient may be defined

$$kA = (k_f A_f + k_t A_t)$$

and

$$q_{ki} = q_{k_{i, i+1}} + q_{k_{i, i-1}} = kA(T_i - T_{i+1})/\Delta z + kA(T_i - T_{i-1})/\Delta z$$

Note that for the top segment, $i = 1$, $q_{k_{i, i-1}} = 0$

and for the N th segment

$$q_{k_{i, i+1}} = 0$$

Energy can also be transferred into and out of a segment due to mass transfer across the segment boundaries. The formulation for this energy transport depends on the location of the segment with respect to the points at which mass is added to the tank and on the relative magnitudes of the collector and load flow rates. The terms accounting for the net energy added to a segment due to mass transfer can be shown using a five segment tank, one segment of each possible type encountered in a storage tank. Taking the normal case where collector return fluid is hotter than load return fluid there will be, as shown in Fig. B2:

segment type	description
1	above collector return
2	collector return
3	between collector and load returns
4	load return
5	below load return

A situation may exist in which one or more of the above segment types are not present and others are combined. For instance, if collector and load return temperatures were equal, both would enter the same segment. In this case there would be no segments of type 3 and segment types 2 and 4 would be combined. Such conditions must be taken into account in the generalized energy equation.

Convective energy transfer can be calculated knowing the collector and load mass flow rates and temperatures and segment temperatures. For collector return temperature greater than load return temperature, convective energy transfer for each segment is listed in Table B1.

Thus, an energy balance may be written for the i th segment

$$M_c \frac{dT_i}{dt} = -q_{ei} - q_{ki} + q_{ci}$$

where q_{ci} depends upon the flow conditions and the segment under consideration.

To facilitate computation, several control functions are introduced. Master on/off controls, F_{CC} and F_{LL} are provided for collector and load loops respectively. Collector return location control F_{i+1}^C is set equal to zero for T_C less than T_i . All other F_i^C are equal to one. The end point values of the function F^C are fixed at $F_1^C = 0$ and $F_{N+1}^C = 1$. Note that the term $F_{i+1}^C (1 - F_i^C)$ is one only for the hottest segment whose temperature is less than or equal to the collector return temperature. This is the segment where collector return fluid is introduced. A similar load return control, F_i^L , is defined. Various combinations of these controls can be used to construct terms which will equal one only for one segment type:

segment type	term
1	$1 - F_{i+1}^C$
2	$F_{i+1}^C (1 - F_i^C)$
3	$F_i^C (1 - F_{i+1}^L)$
4	$F_{i+1}^L (1 - F_i^L)$
5	F_i^L

Two additional controls, F^{LC} and F^{CL} , are set equal to one for load mass flow rate greater than collector mass flow rate and for collector mass flow rate greater than load mass flow rate respectively.

Using the Euler approximation, the energy equation for the i th segment for T_c greater than T_e becomes

$$\begin{aligned}
& \dot{m}_{c,p} F_{i+1}^{CC} F_i^C (1 - F_i^C) T_c + \dot{m}_{e,p} F_{i-1}^{LL} F_i^L (1 - F_i^L) T_e \\
& + \dot{m}_{e,p} F_{i-1}^{LL} (1 - F_i^C) [(1 - F_{i+1}^C) T_{i+1} - T_i] \\
& + \dot{m}_{c,p} F_{i+1}^{CC} F_i^L (F_i^L T_{i-1} - T_i) \\
& + (\dot{m}_e F_{i-1}^{LL} - \dot{m}_c F_{i+1}^{CC}) F_{i+1}^C (1 - F_i^L) [(1 - F_{i+1}^L) F^{LC} T_{i+1} \\
& \quad - F^{LC} F_i^C T_i + F^{CL} (1 - F_{i+1}^L) T_i - F^{CL} F_i^C T_{i-1}] \\
& + (UA_s)_i (T_a - T_i) \\
& + kA(T_{i-1} - T_i)/\Delta z + kA(T_{i+1} - T_i)/\Delta z \\
& = \dot{M} c_p \Delta T_i / \Delta t
\end{aligned}$$

Following a similar analysis for T_e greater than T_c the equation becomes

$$\begin{aligned}
& \dot{m}_{c,p} F_{i+1}^{CC} F_i^C (1 - F_i^C) T_c + \dot{m}_{e,p} F_{i+1}^{LL} F_i^L (1 - F_i^L) T_e \\
& + \dot{m}_{e,p} F_{i+1}^{LL} (1 - F_i^L) [(1 - F_{i+1}^L) T_{i+1} - T_i] \\
& + \dot{m}_{c,p} F_{i+1}^{CC} F_i^C (F_i^C T_{i+1} - T_i)
\end{aligned}$$

$$\begin{aligned}
& + (UA_s)_i (T_a - T_i) \\
& + kA(T_{i+1} - T_i)/\Delta z + kA(T_{i-1} - T_i)/\Delta z \\
& = Mc_p \Delta T_i / \Delta t
\end{aligned}$$

NOMENCLATURE FOR APPENDIX B.

- A_f - cross-sectional area of the fluid
- A_t - cross-sectional area of the tank walls
- $(UA_s)_i$ - total conductance between segment i and environment
- c_p - specific heat of the fluid
- F^C - collector return location control
- F^{CC} - collector ON/OFF control
- F^{CL} - control, 1 for $\dot{m}_c > \dot{m}_\ell$, zero otherwise
- F^L - load return location control
- F^{LC} - control, 1 for $\dot{m}_\ell > \dot{m}_c$, zero otherwise
- F^{LL} - load ON/OFF control
- k_f - thermal conductivity of the fluid
- K_t - thermal conductivity of the tank walls
- kA - overall conductance between segments
- M - mass of the segment
- N - number of tank segments
- \dot{m}_c - collector mass flow rate
- \dot{m}_ℓ - load mass flow rate
- q_c - convective energy transfer
- q_e - energy transfer to environment
- q_k - conductive energy transfer within tank
- q_k - conductive energy transfer to segment below
 $i, i+1$

- q_k - conductive energy transfer to segment above
- $i, i-1$
- T_i - segment temperature, $i = 1$ at top, $i = N$ at bottom
- T_c - collector return temperature
- T_ℓ - load return temperature
- T_a - environment temperature
- t - time
- Δt - time step
- z - vertical coordinate
- Δz - distance between segments

TABLE I

Base System Parameters

Storage Tank

volume	4.0 m ³ (1057 gal H ₂ O)
height/diameter	2.0
wall thickness	.0015 m (.060 in)
wall conductivity	171.4 $\frac{\text{KJ}}{\text{m}^2\text{hr}^\circ\text{C}}$ (27.5 $\frac{\text{Btu}}{\text{hrft}^\circ\text{C}}$)
top loss coef	1.6 $\frac{\text{KJ}}{\text{m}^2\text{hr}^\circ\text{C}}$ (.0783 $\frac{\text{Btu}}{\text{ft}^2\text{hr}^\circ\text{F}}$)
side loss coef	1.6 $\frac{\text{KJ}}{\text{m}^2\text{hr}^\circ\text{C}}$ (.0783 $\frac{\text{Btu}}{\text{ft}^2\text{hr}^\circ\text{F}}$)
bottom loss coef	1.6 $\frac{\text{KJ}}{\text{m}^2\text{hr}^\circ\text{C}}$ (.0783 $\frac{\text{Btu}}{\text{ft}^2\text{hr}^\circ\text{F}}$)
number of segments	20

Storage Fluid

density	1000.0 $\frac{\text{Kg}}{\text{m}^3}$ (62.4 $\frac{\text{lb}}{\text{ft}^3}$)
specific heat	4.19 $\frac{\text{KJ}}{\text{kg}^\circ\text{C}}$ (1.0 $\frac{\text{Btu}}{\text{lb}^\circ\text{F}}$)
conductivity	2.1456 $\frac{\text{KJ}}{\text{m}^2\text{hr}^\circ\text{C}}$ (.3444 $\frac{\text{Btu}}{\text{ft}^2\text{hr}^\circ\text{F}}$)
collector mass flowrate	2500.0 $\frac{\text{Kg}}{\text{hr}}$ (11.01 gpm)
load mass flowrate	2500.0 $\frac{\text{Kg}}{\text{hr}}$ (11.01 gpm)
reference tank temp	40.0°C (104.0°F)
initial tank temp	50.0°C (122.0°F)

Load

UA	1000.0 $\frac{\text{KJ}}{\text{hr}^\circ\text{C}}$ (526.6 $\frac{\text{Btu}}{\text{hr}^\circ\text{F}}$)
room temp	20.0°C (68.0°F)
Heat exchanger efficiency	1.0
load side mass flowrate	2500.0 $\frac{\text{Kg}}{\text{hr}}$ (1222 cfm)
load side fluid specific heat	1.012 $\frac{\text{KJ}}{\text{Kg}^\circ\text{C}}$ (.2415 $\frac{\text{Btu}}{\text{lb}^\circ\text{F}}$)

Minimum load side fluid outlet temp 40.0°C (104.0°F) mode 4

Collector

area 75.0 m² (807 ft²)

F' .876

(τα) .84

U_L 17.9 $\frac{\text{KJ}}{\text{m}^2\text{hr}^\circ\text{C}}$ (.876 $\frac{\text{Btu}}{\text{ft}^2\text{hr}^\circ\text{F}}$)

Simulation

total length 168.0 hr

computation increment .04 hr

output increment 1.0 hr

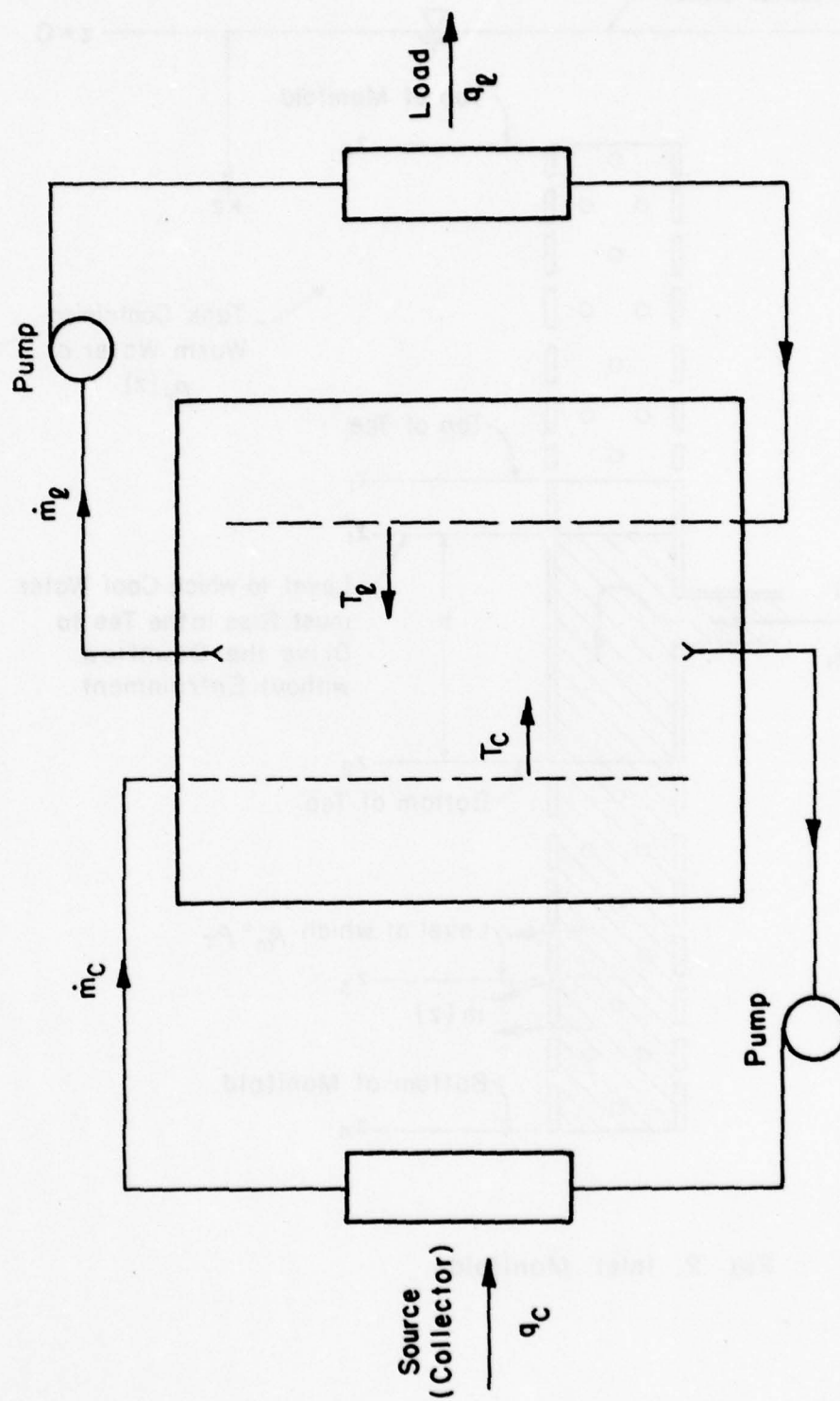


Fig. 1. Stratified Storage System with Variable Tank Inlet Conditions

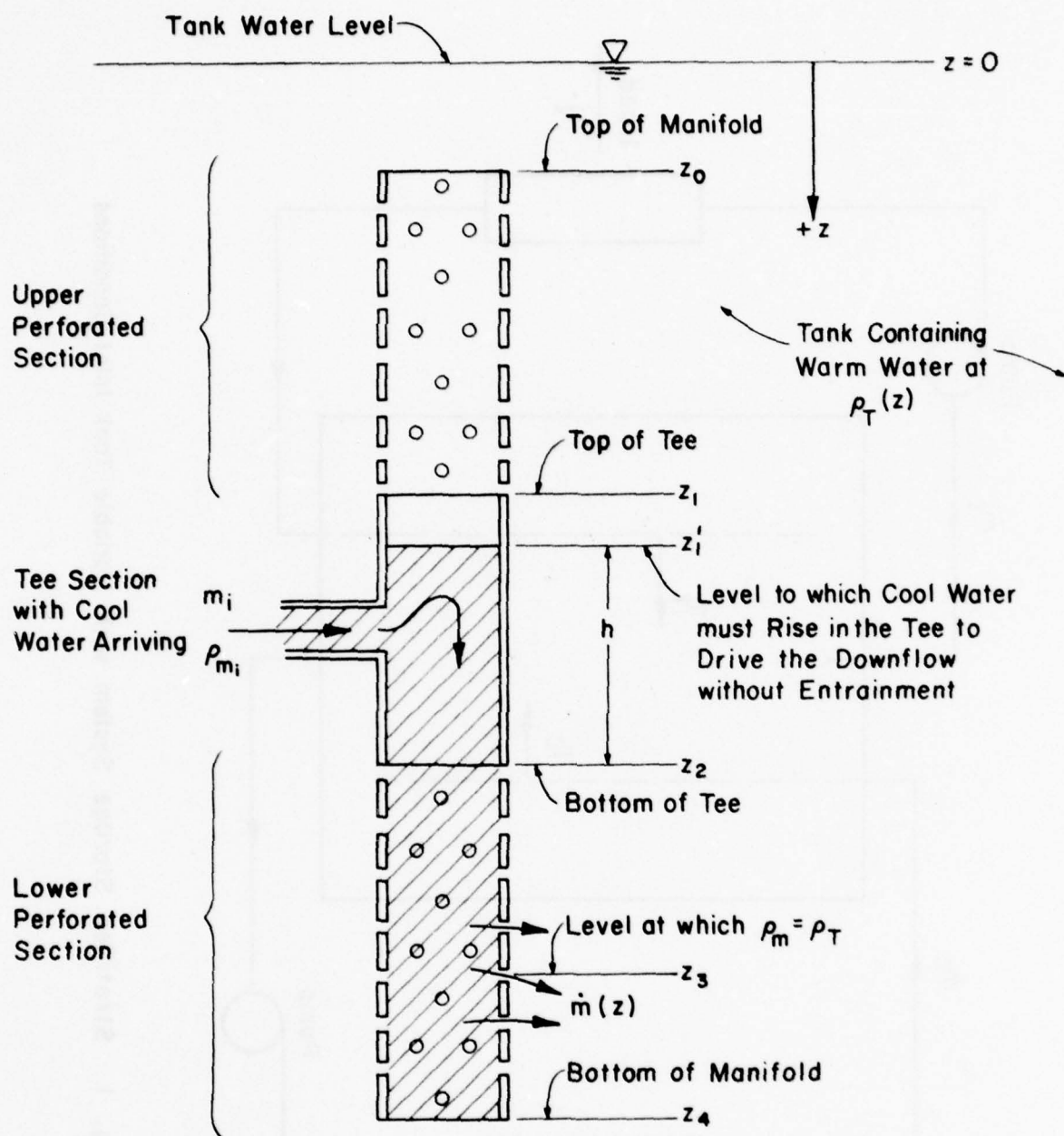


Fig. 2. Inlet Manifold

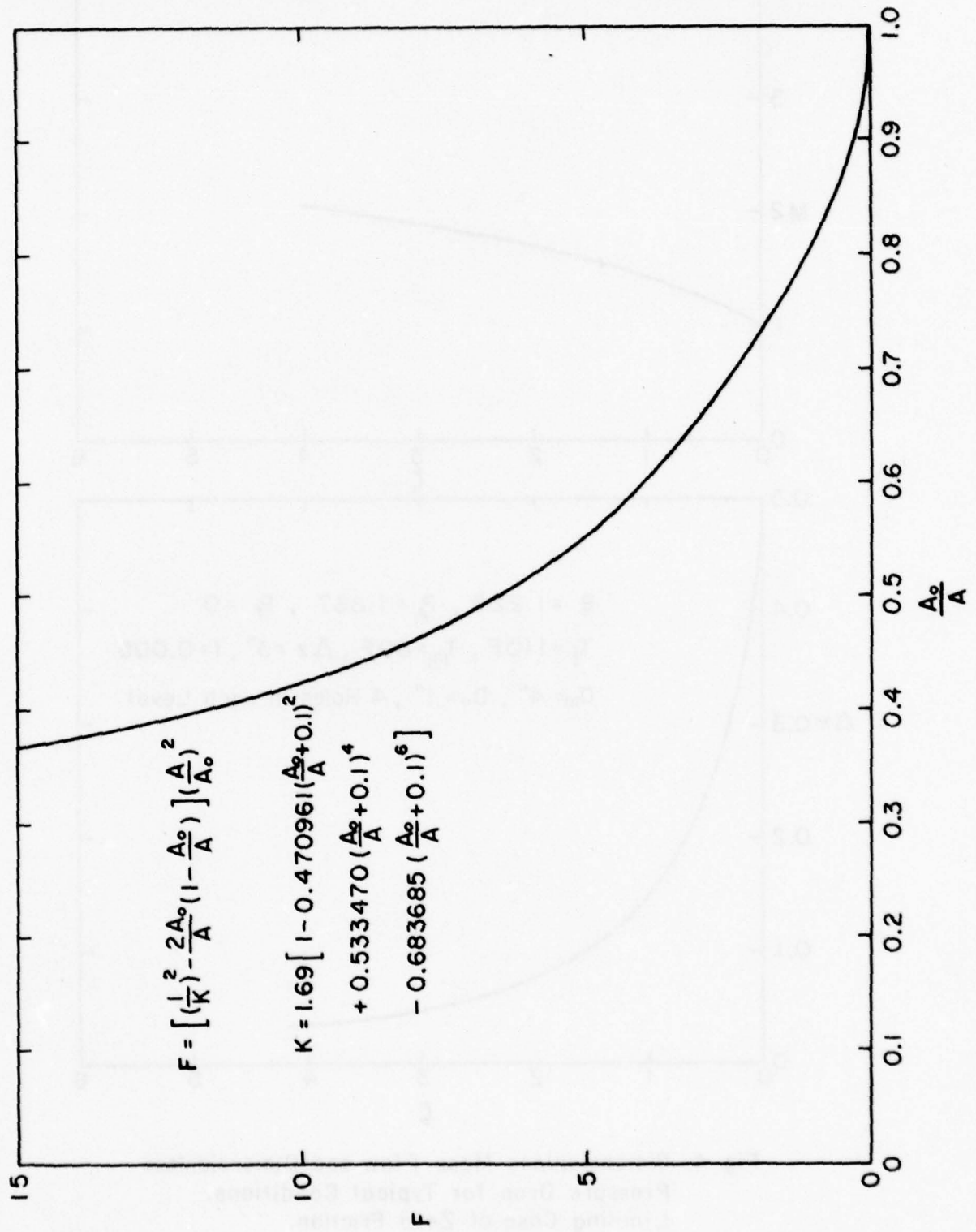


Fig. 3. F vs A_o/A for Orifice-like Resistance Elements

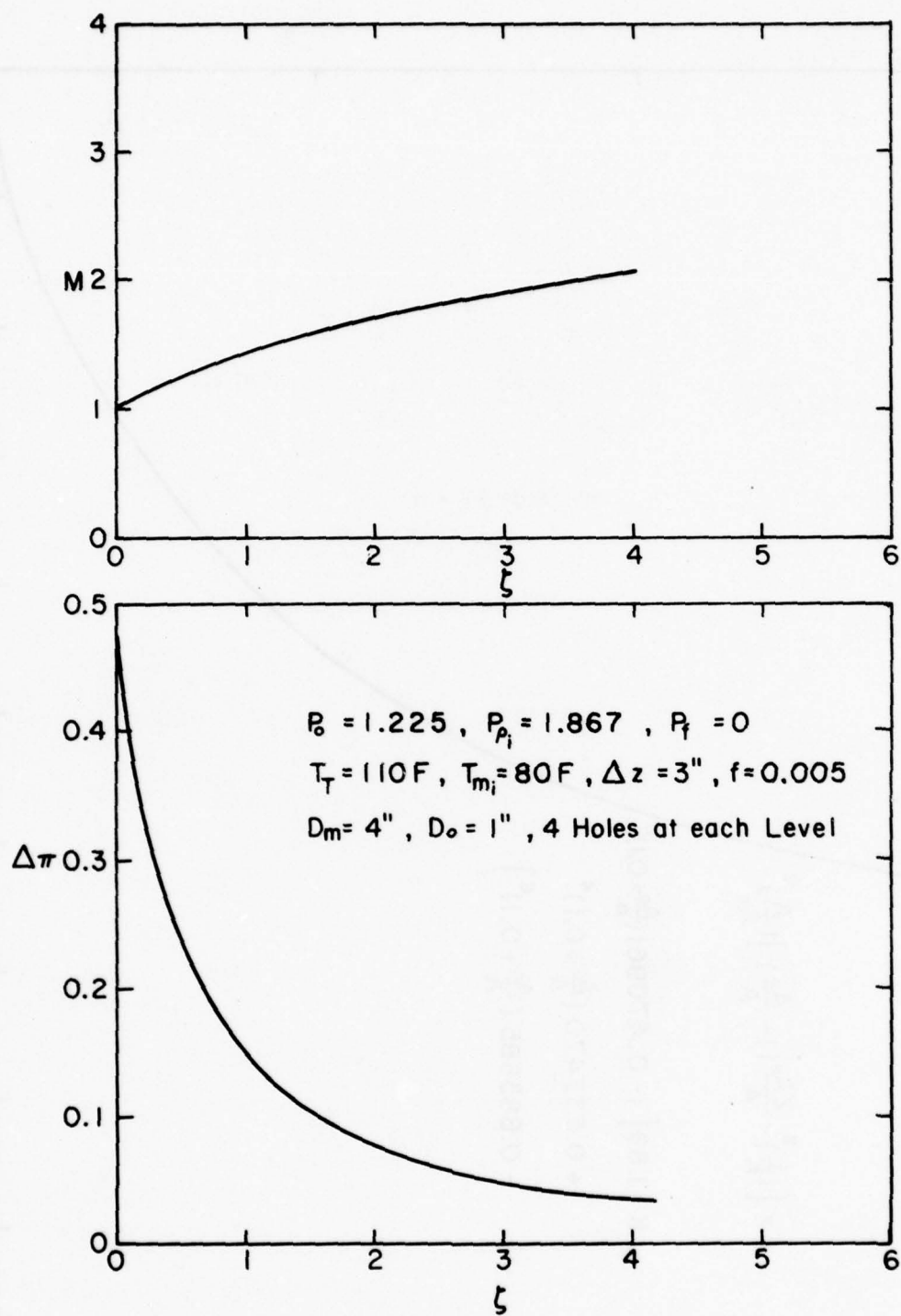
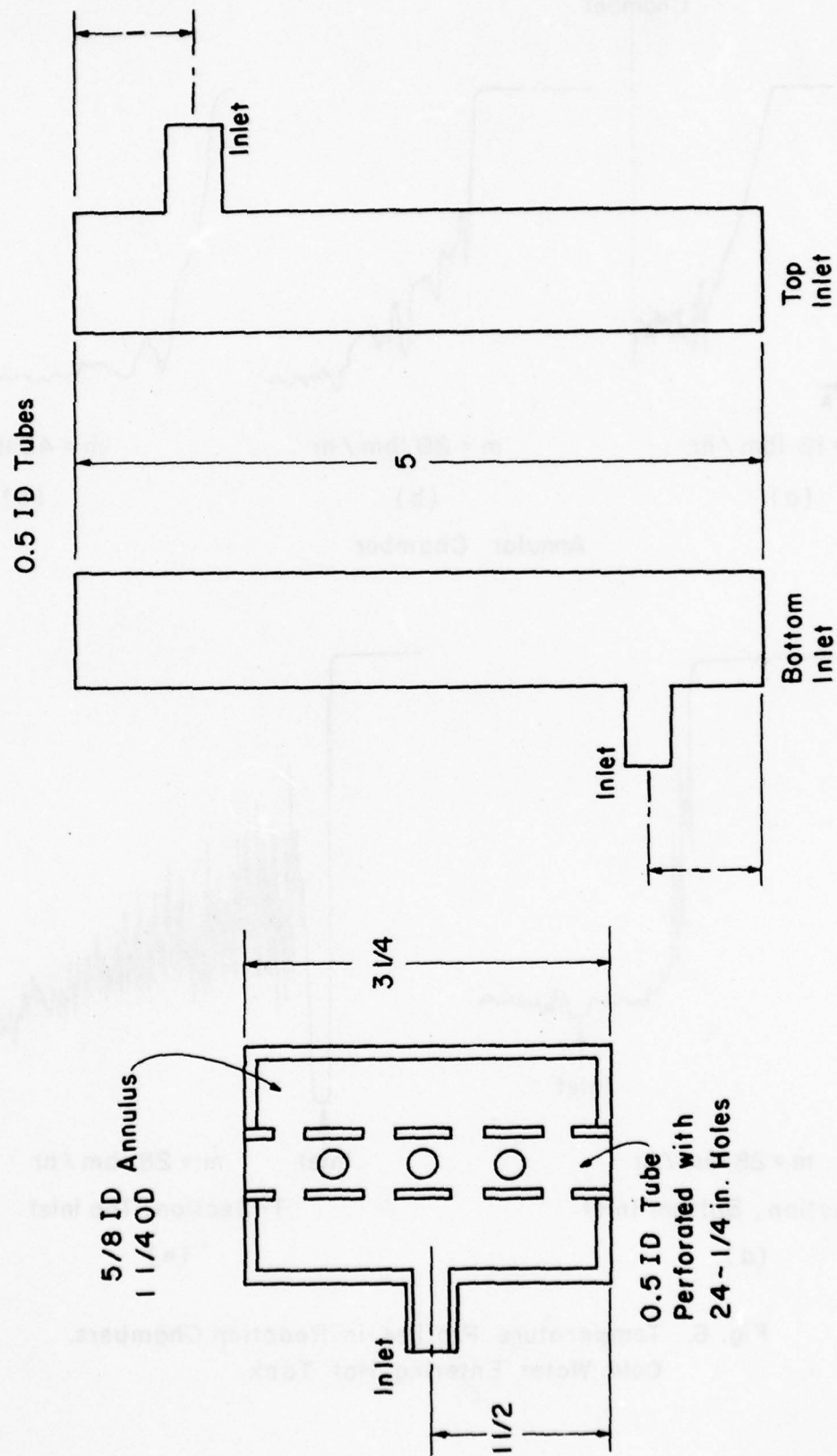


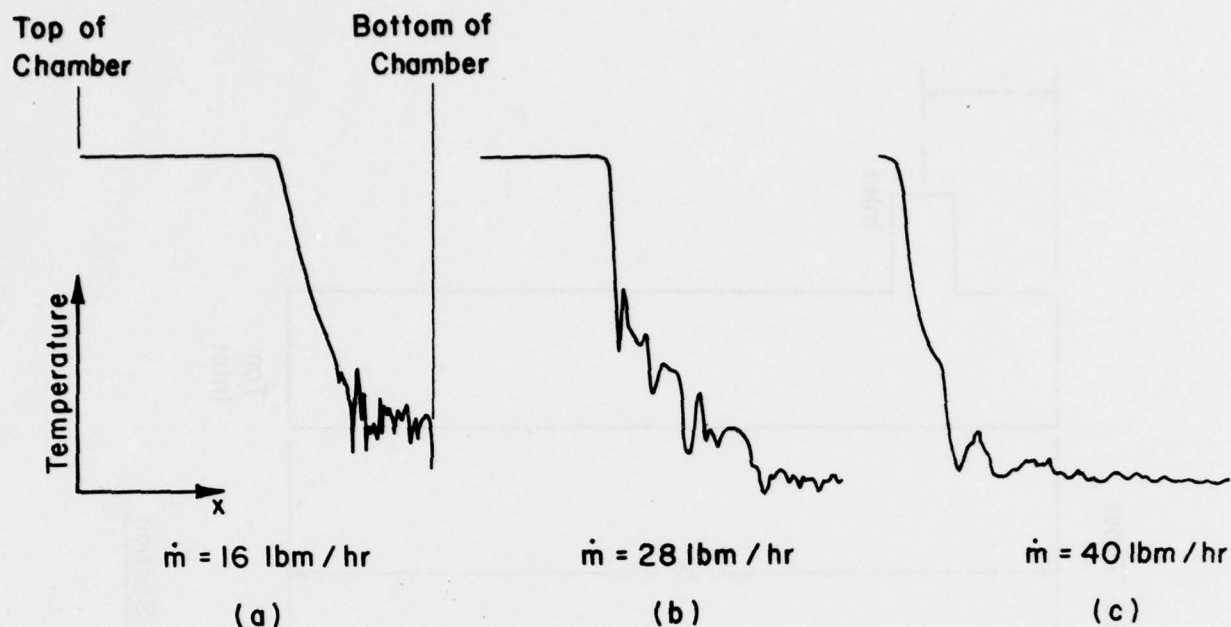
Fig. 4. Dimensionless Mass Flow and Dimensionless Pressure Drop for Typical Conditions. Limiting Case of Zero Friction.



Annular

T - Section

Fig. 5. Plexiglas Reaction Chambers.
Dimensions in inches.



Annular Chamber

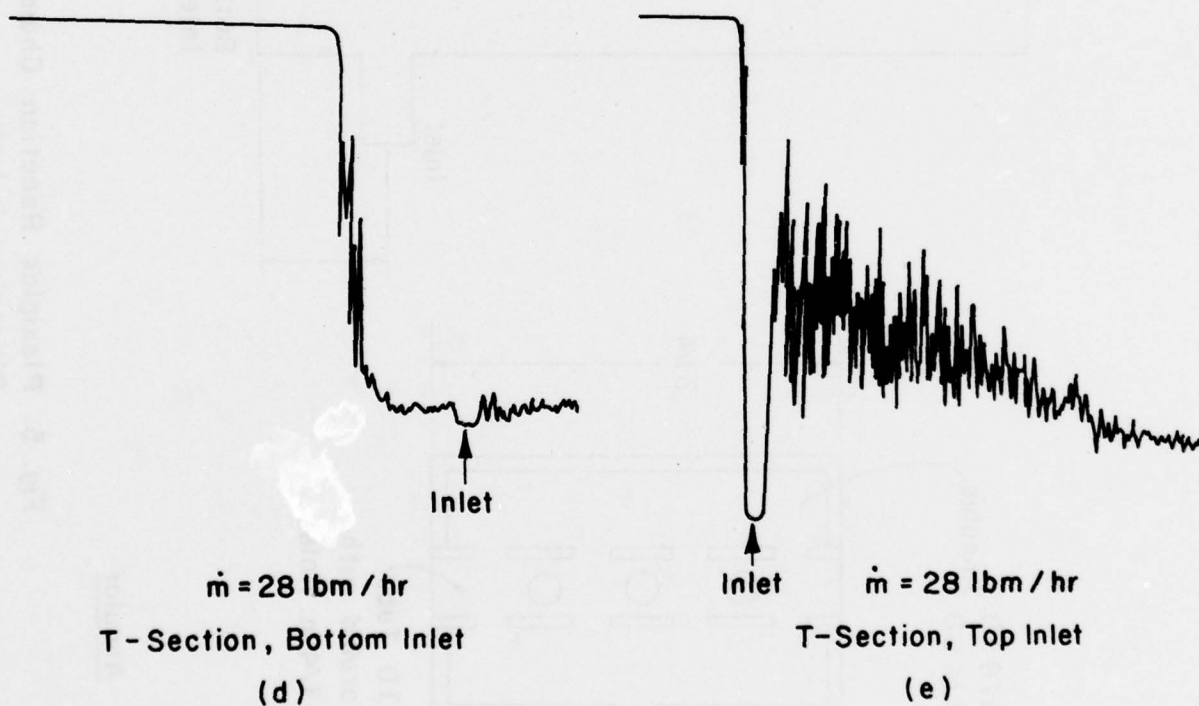


Fig. 6. Temperature Profiles in Reaction Chambers.
Cold Water Entering Hot Tank.

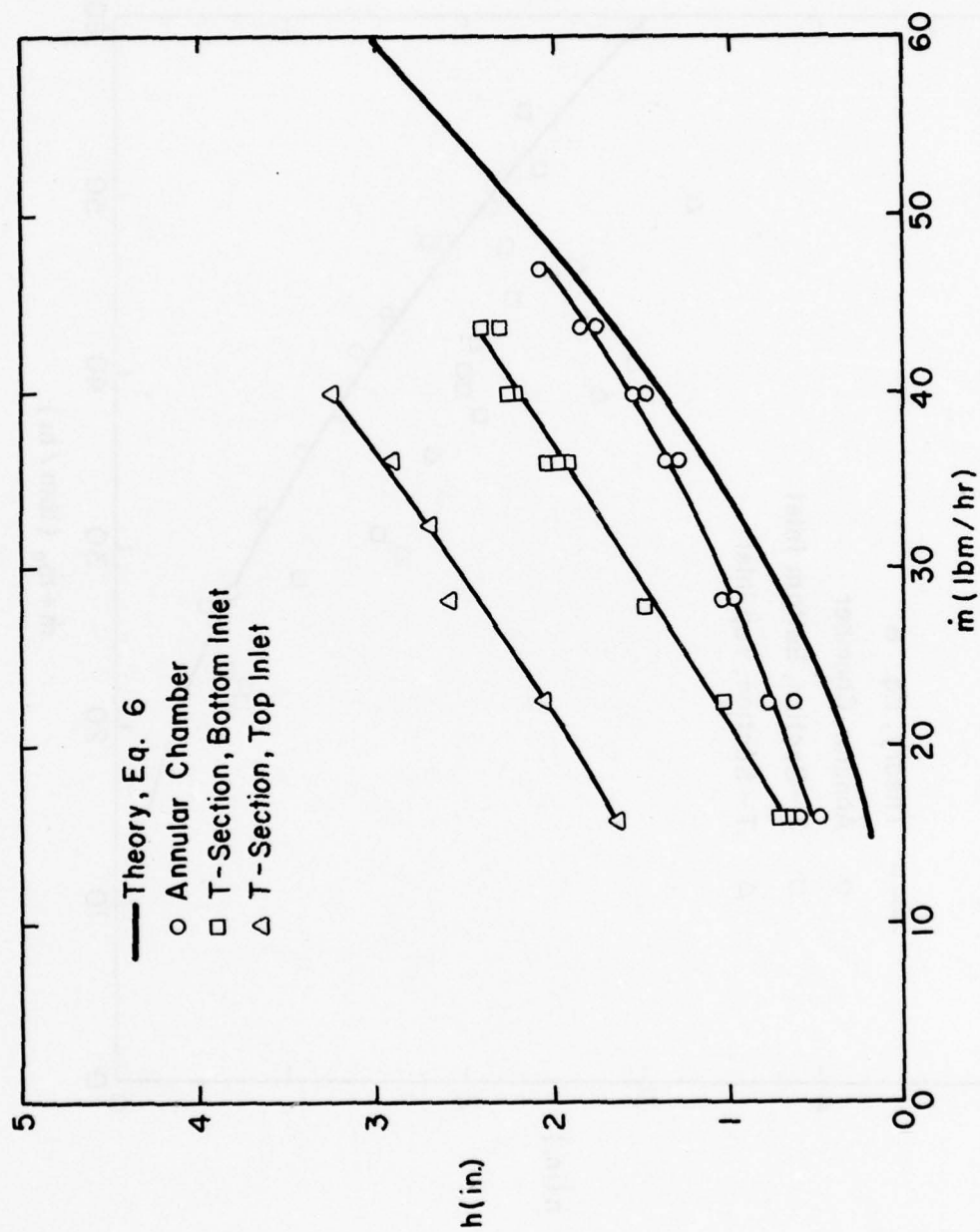


Fig. 7. Location of Interface in Reaction Chambers

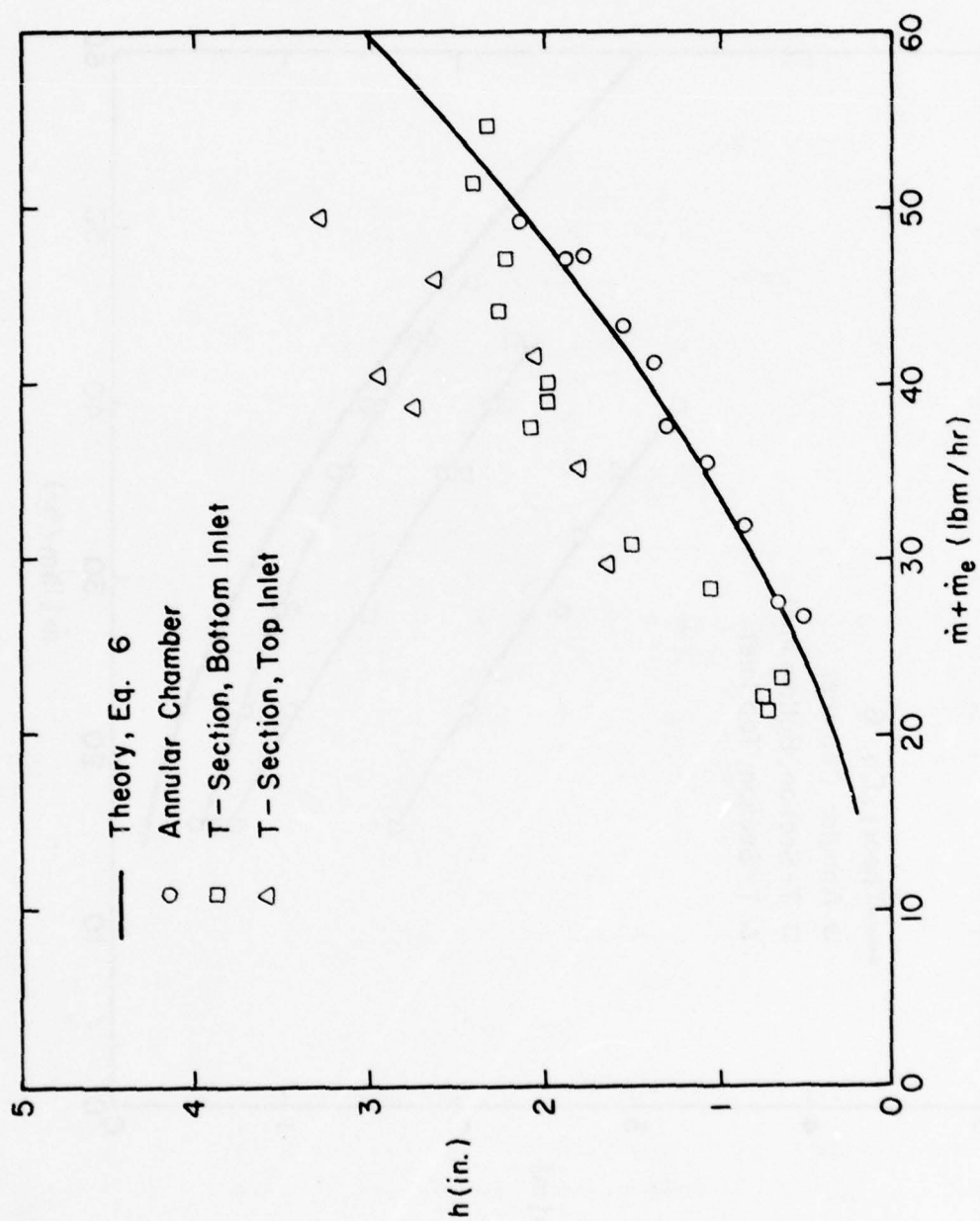


Fig. 8. Location of Interface in Reaction Chambers

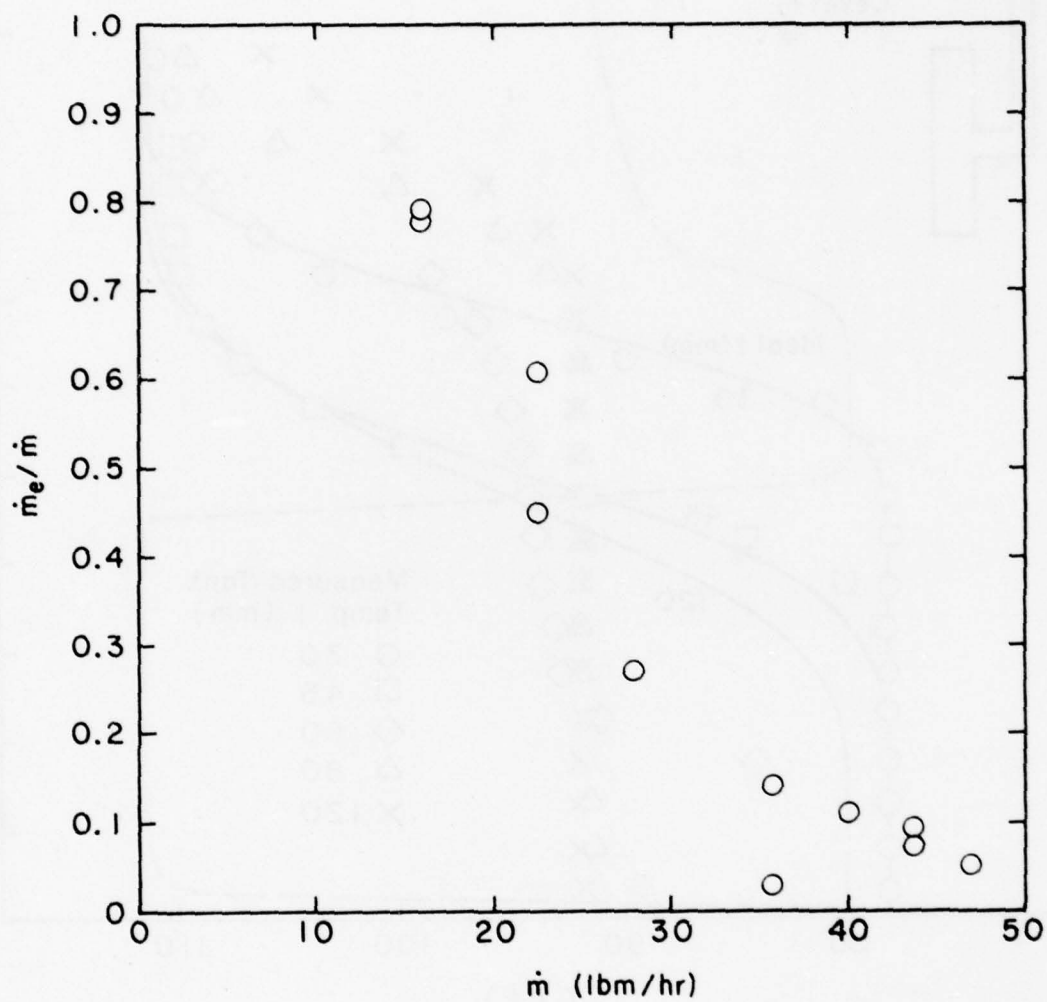


Fig. 9. Ratio of Entrainment Flow Rate to Inlet Flow Rate for Annular Chamber

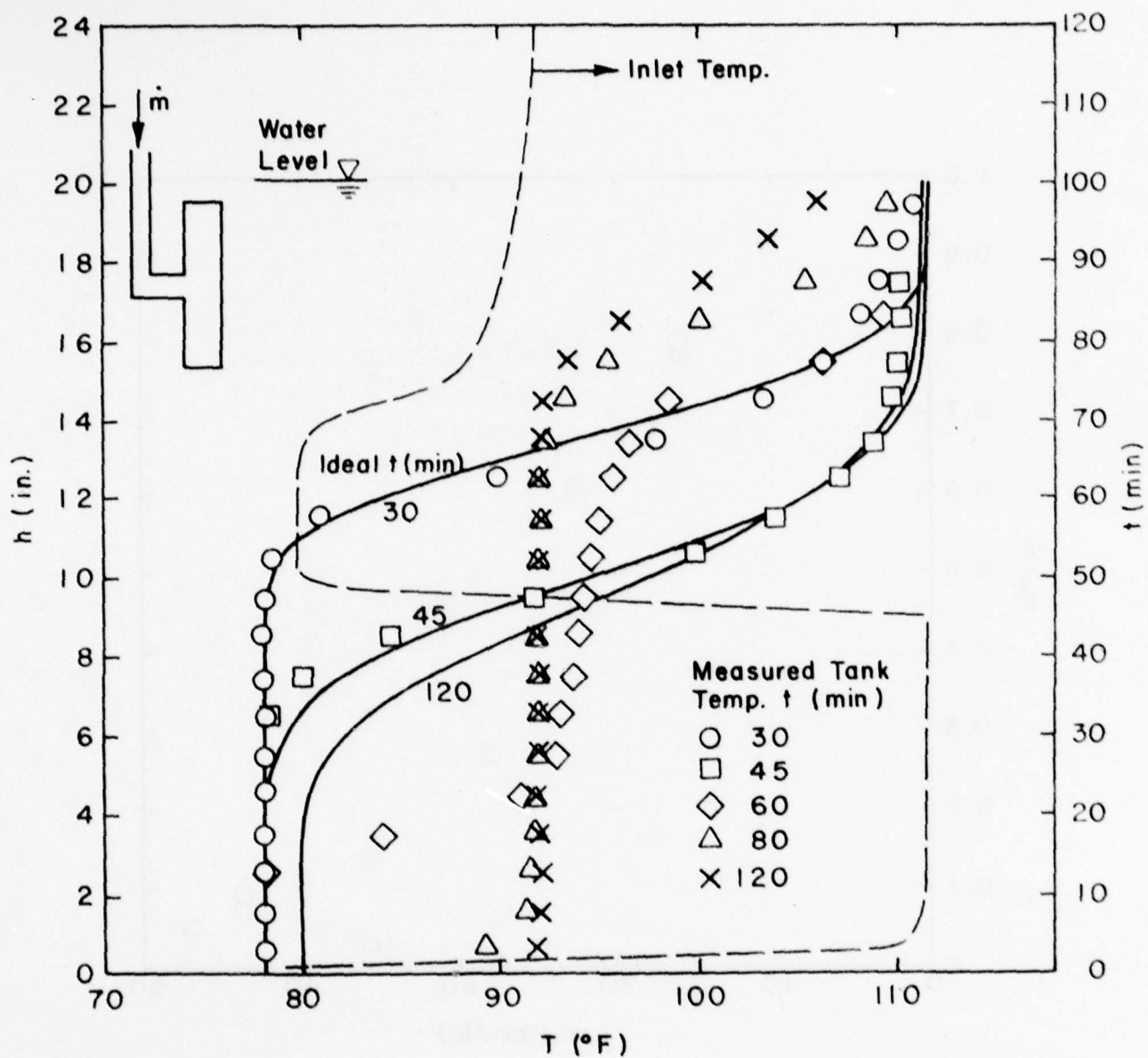


Fig. 10. Tank Temperature Profiles and Inlet Temperature History. Annular Reaction Chamber Alone.

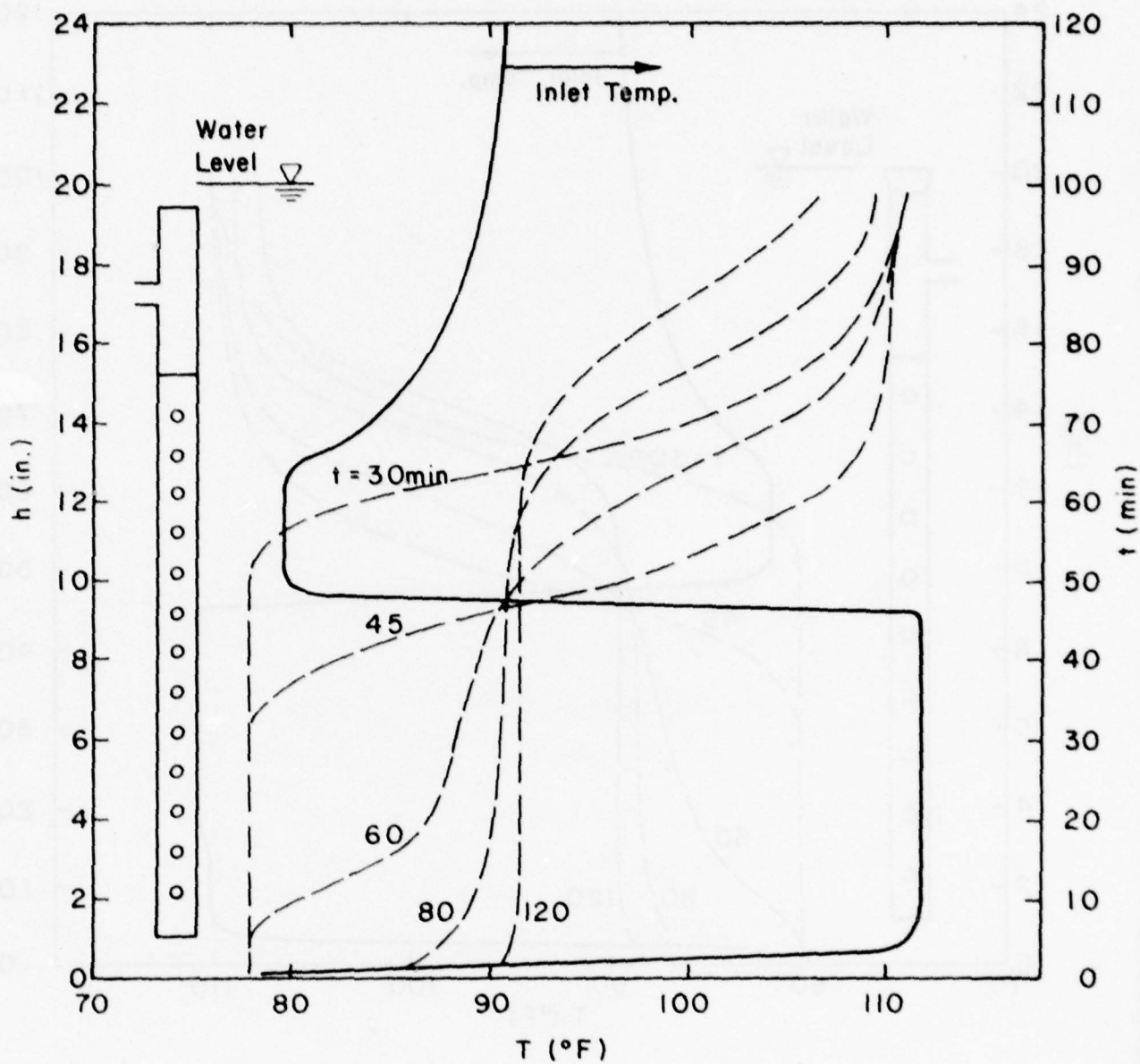


Fig. 11. Tank Temperature Profiles and Inlet Temperature History. 1 1/2 I.D. Manifold. 4 - 1/4 in. Perforations on 1/2 in. Spacing.

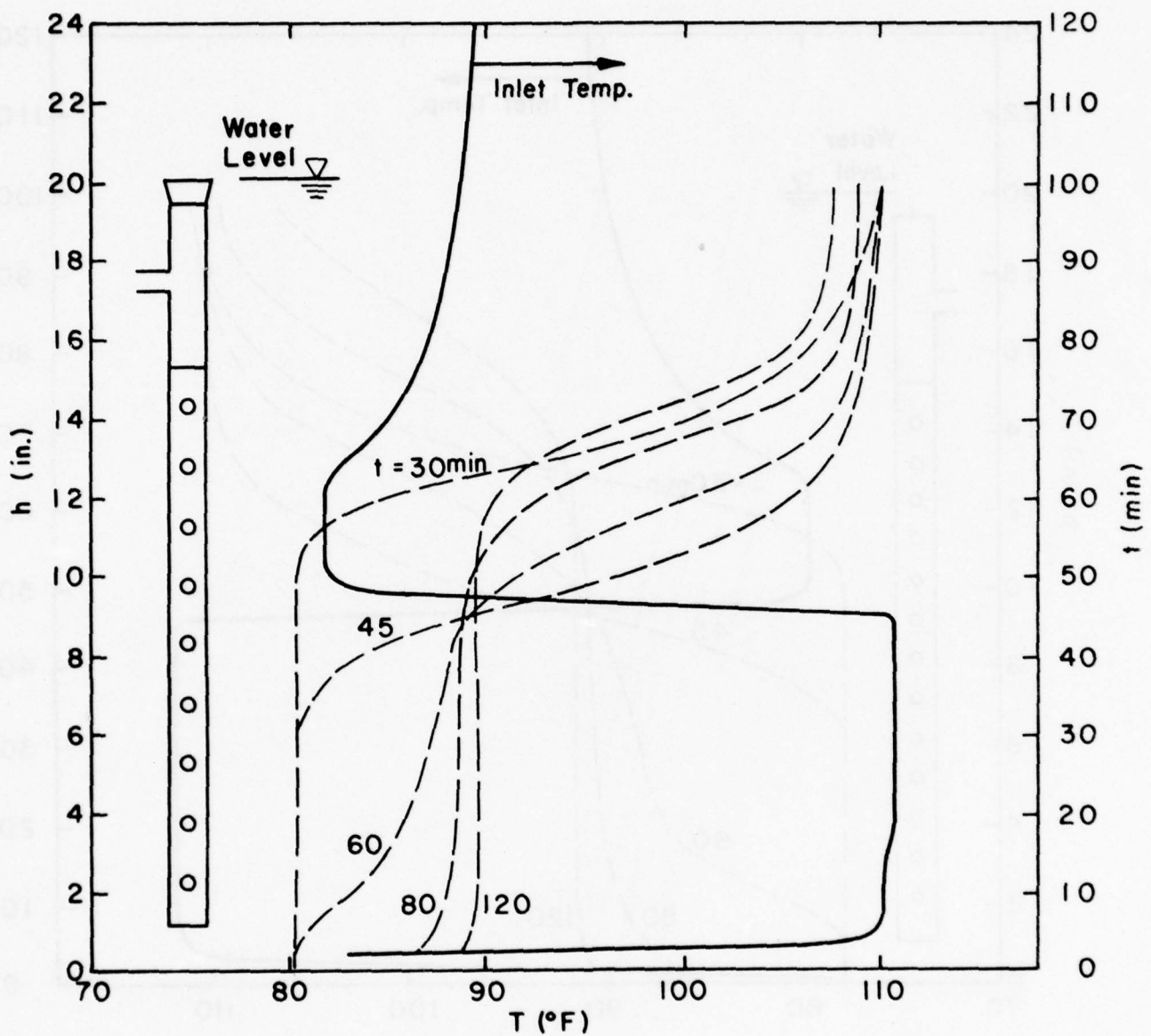


Fig. 12. Tank Temperature Profiles and Inlet Temperature History. Top of Reaction Chamber Sealed at $t = 45$ min.

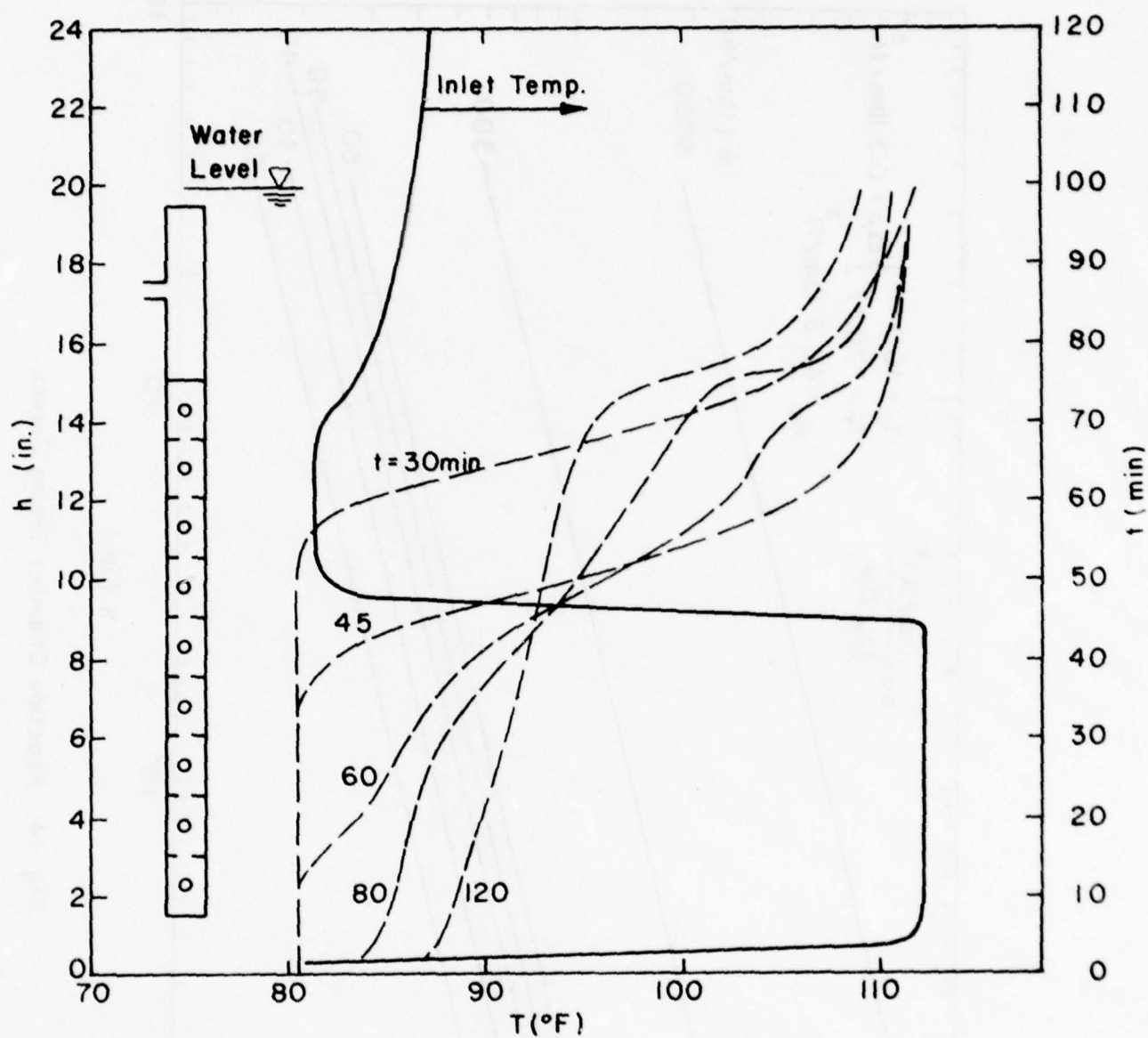


Fig. 13. Tank Temperature Profiles and Inlet Temperature History. Ten Equally Spaced Resistance Elements. 1in. I.D. \times 1 3/8in. O.D.

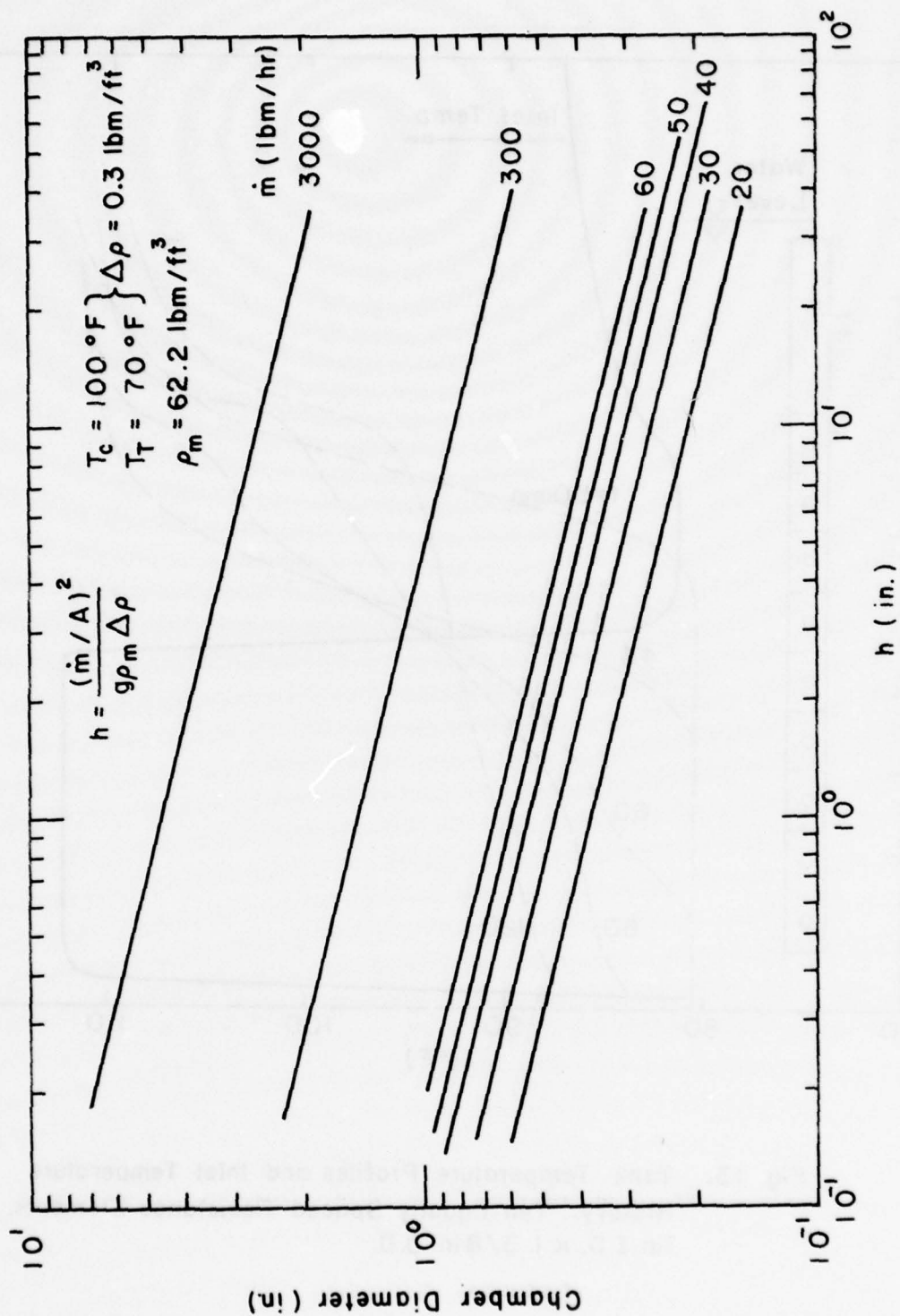


Fig. 14. Reaction Chamber Sizing Curves

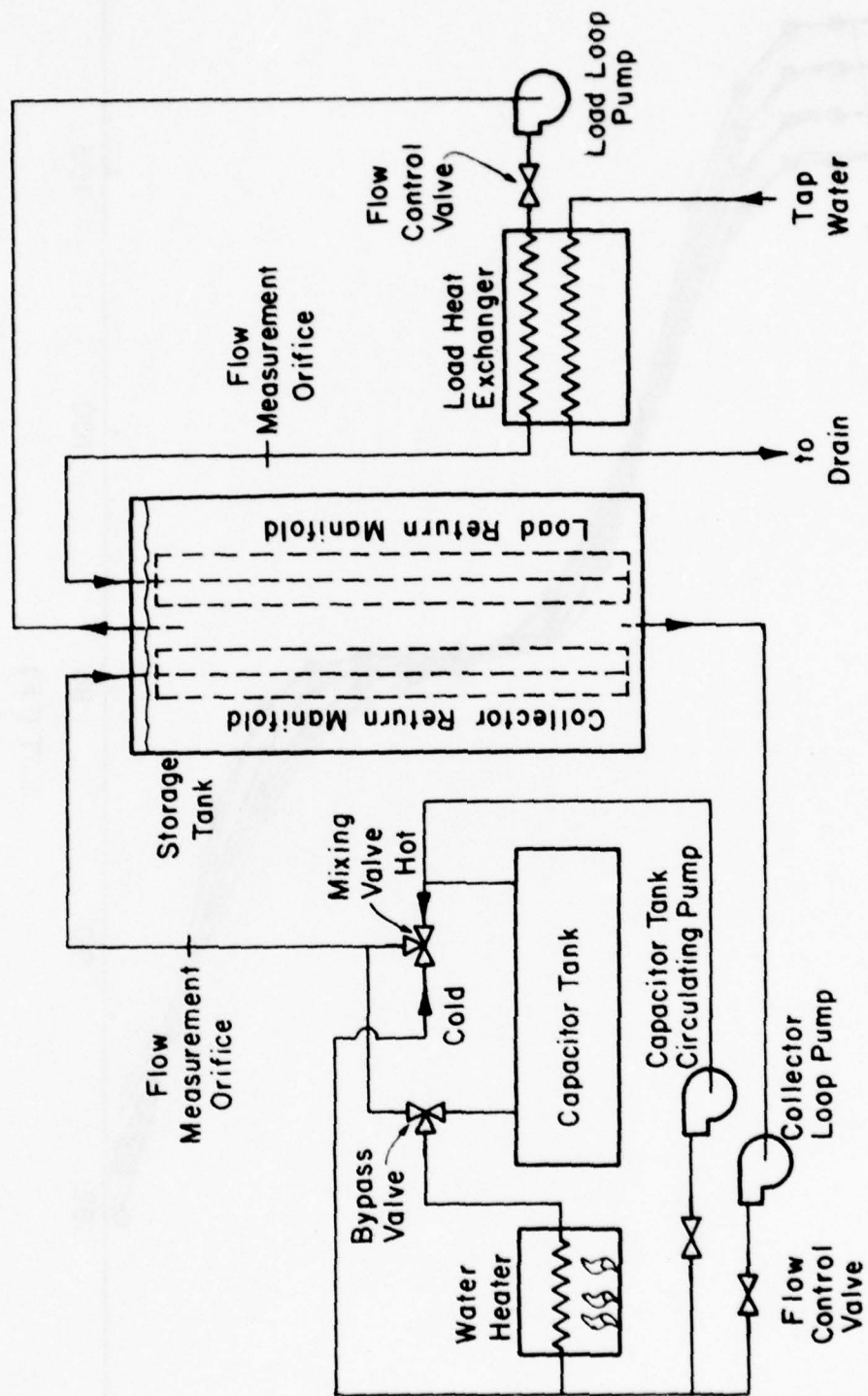


Fig. 15. Prototype System Schematic

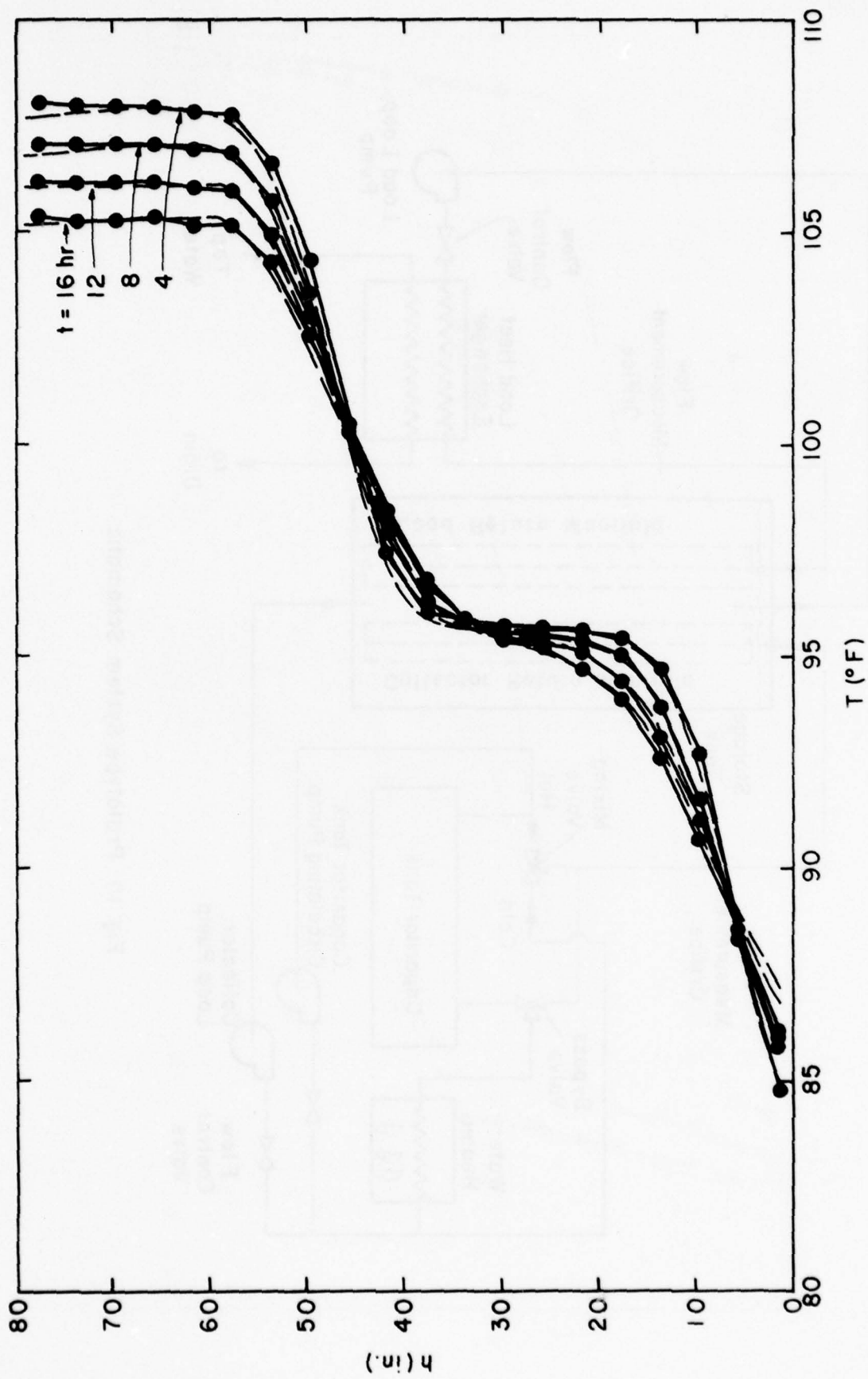


Fig. 16. Tank Temperature Profiles, No Flow

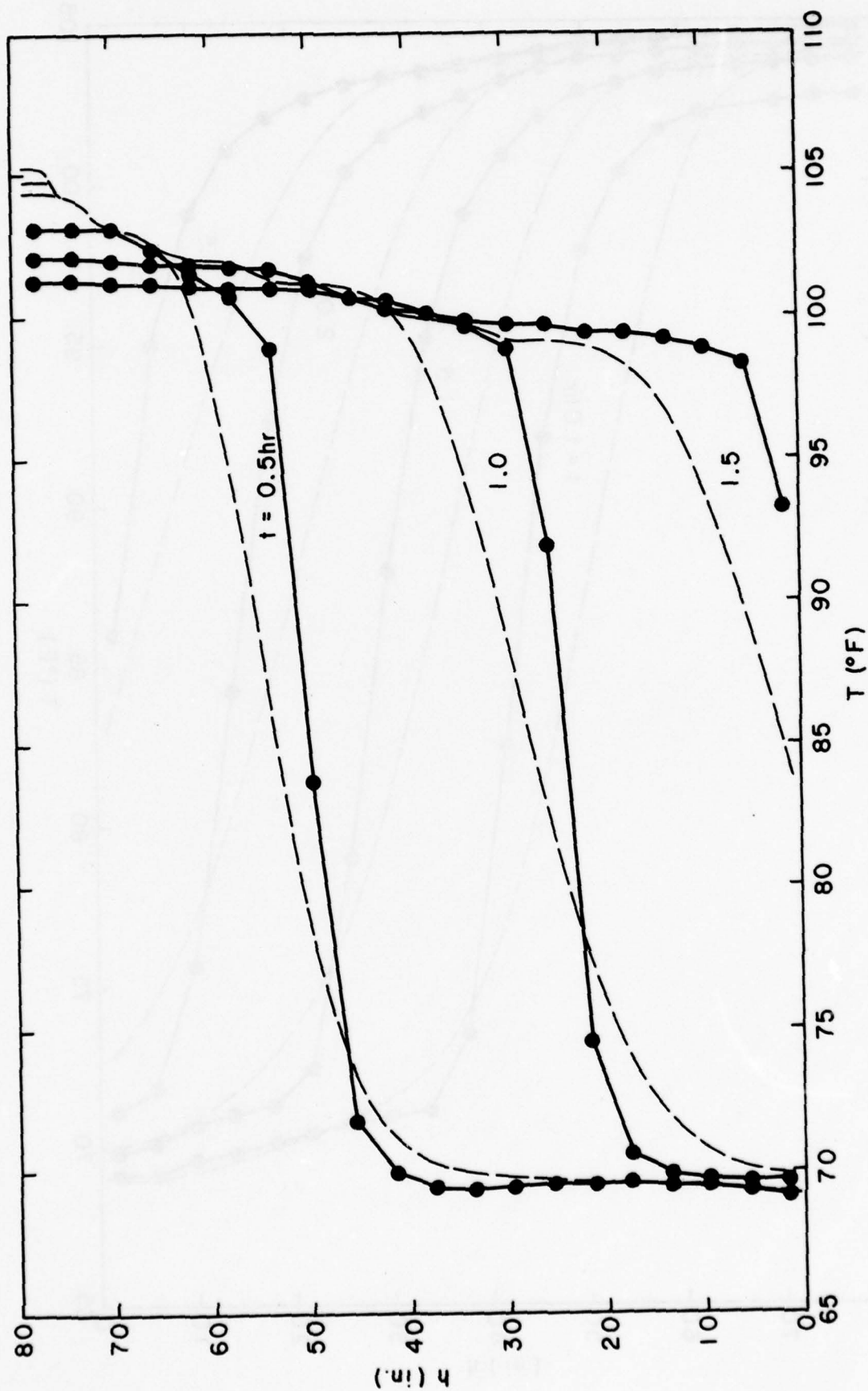


Fig. 17. Tank Temperature Profiles, Charging $\dot{m}_c = 3000 \text{ lbm/hr}$

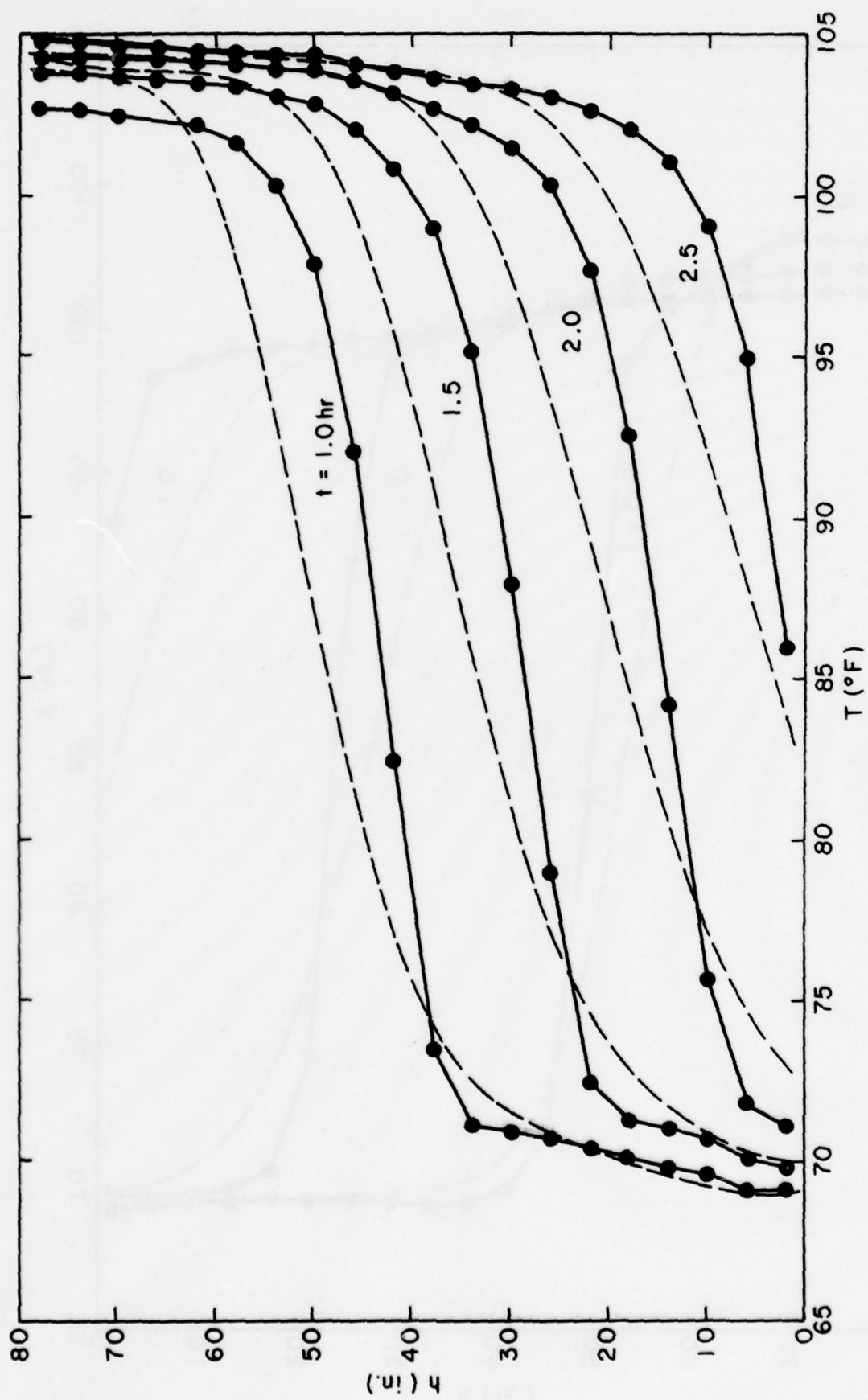


Fig. 18. Tank Temperature Profiles, Charging $\dot{m}_c = 1750$ lbm/hr

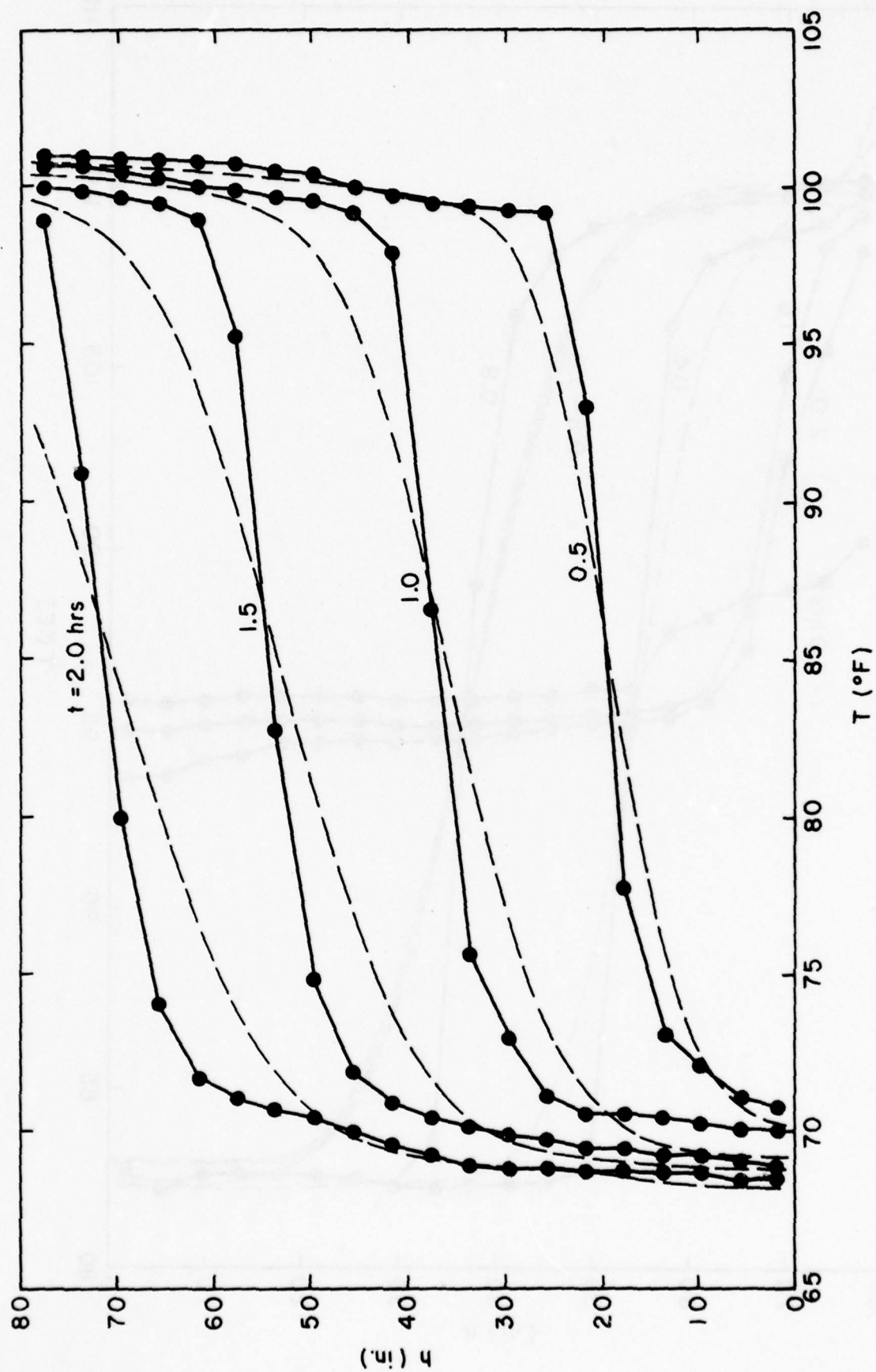


Fig. 19. Tank Temperature Profiles, Discharging $\dot{m}_g = 2020 \text{ lbm/hr}$

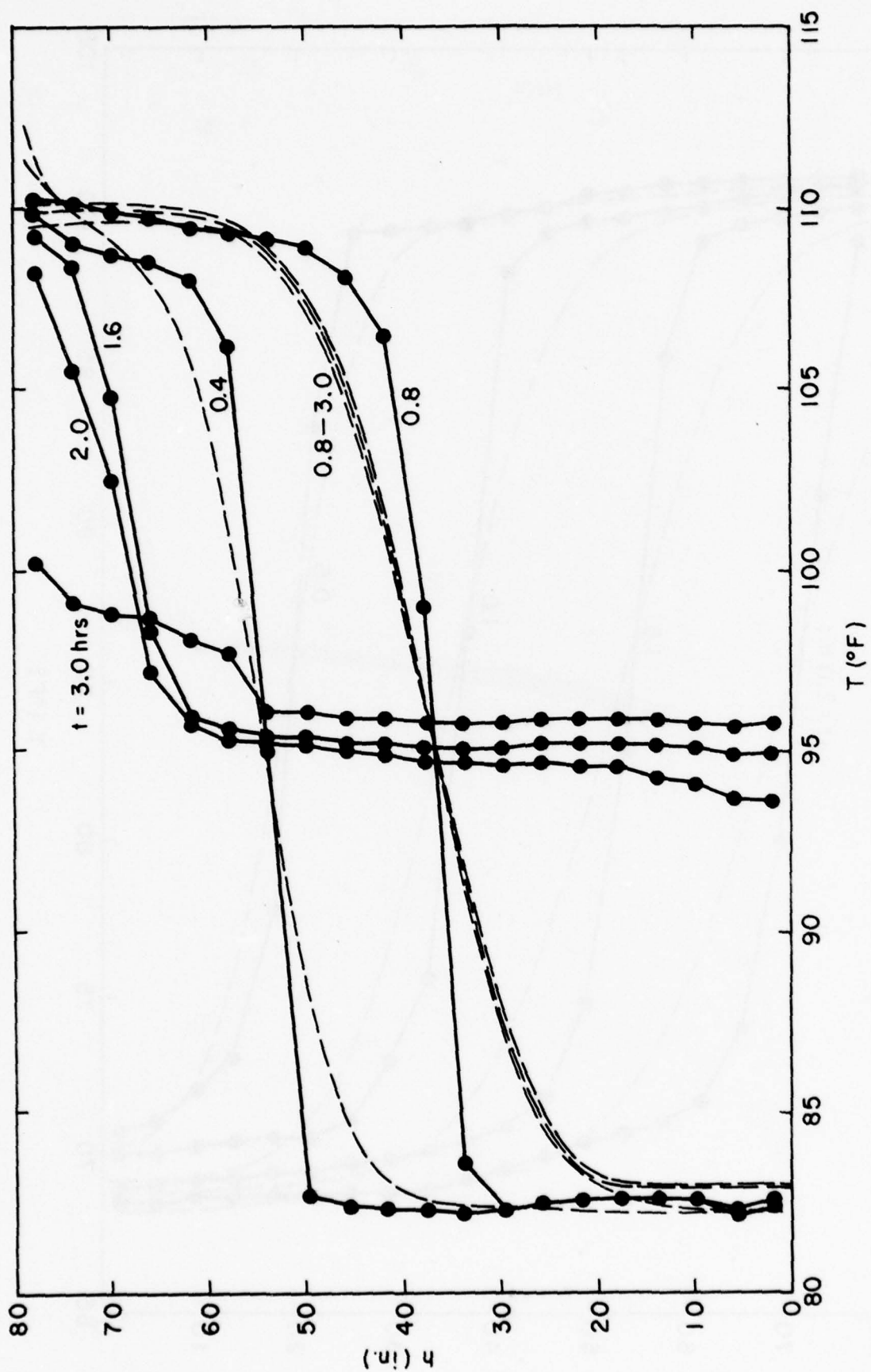


Fig. 20. Partial Charge and Recycle, $\dot{m}_c = 3100$ lbm/hr

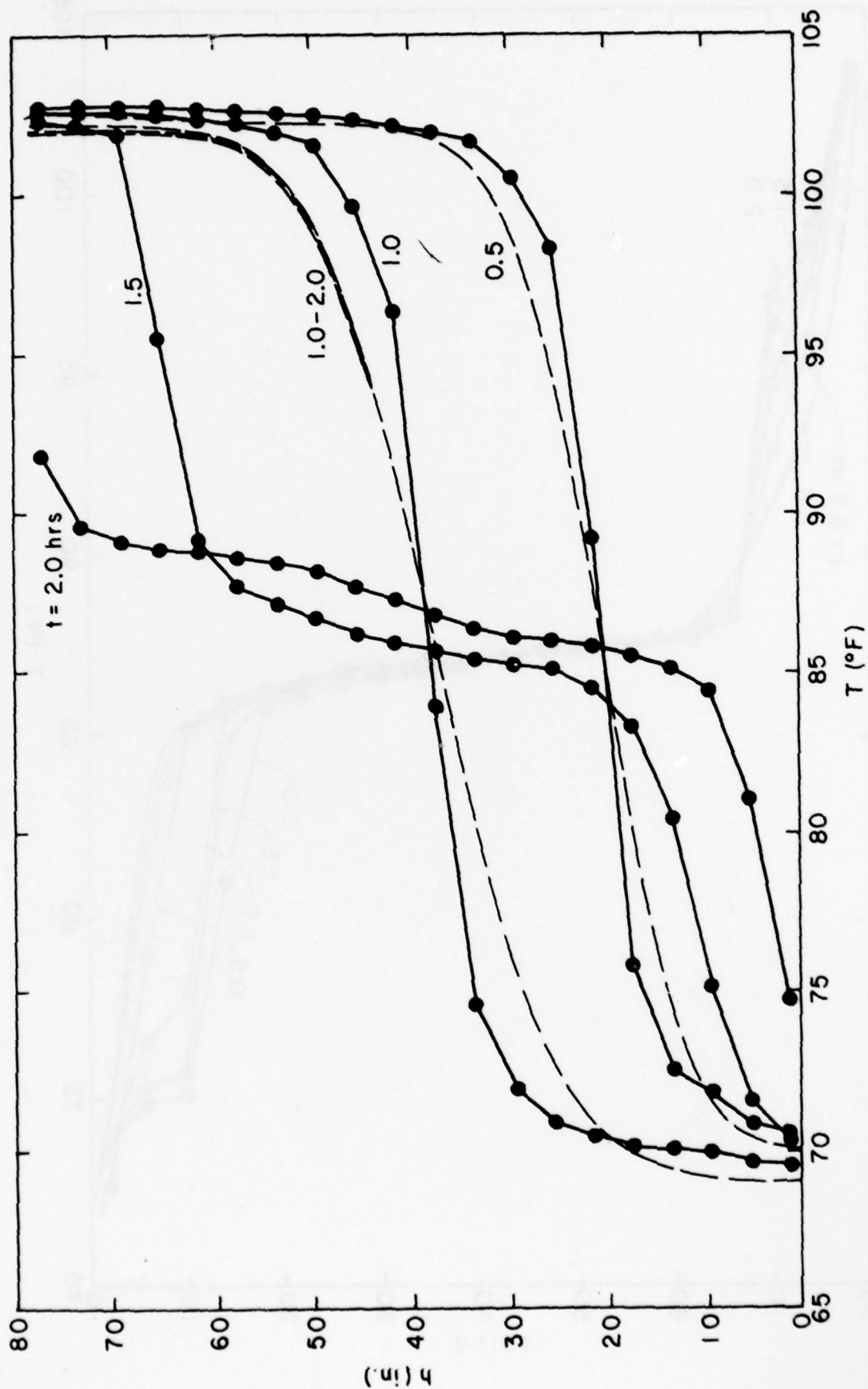


Fig. 21. Partial Discharge and Recycle, $\dot{m}_g = 2000$ lbm / hr

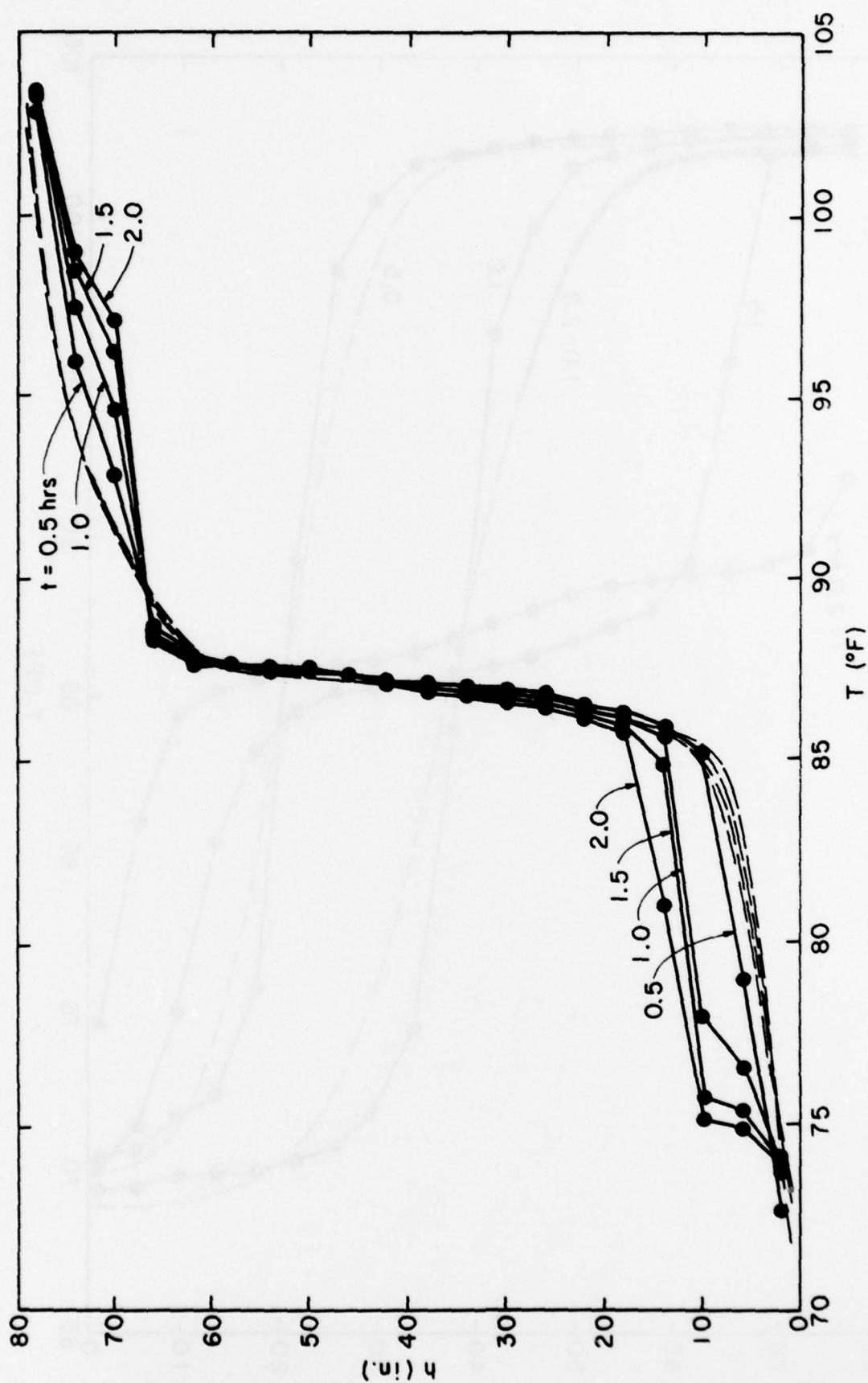


Fig. 22. Simultaneous Charge and Discharge, $\dot{m}_c = 2000$, $\dot{m}_d = 2020$ lbm / hr

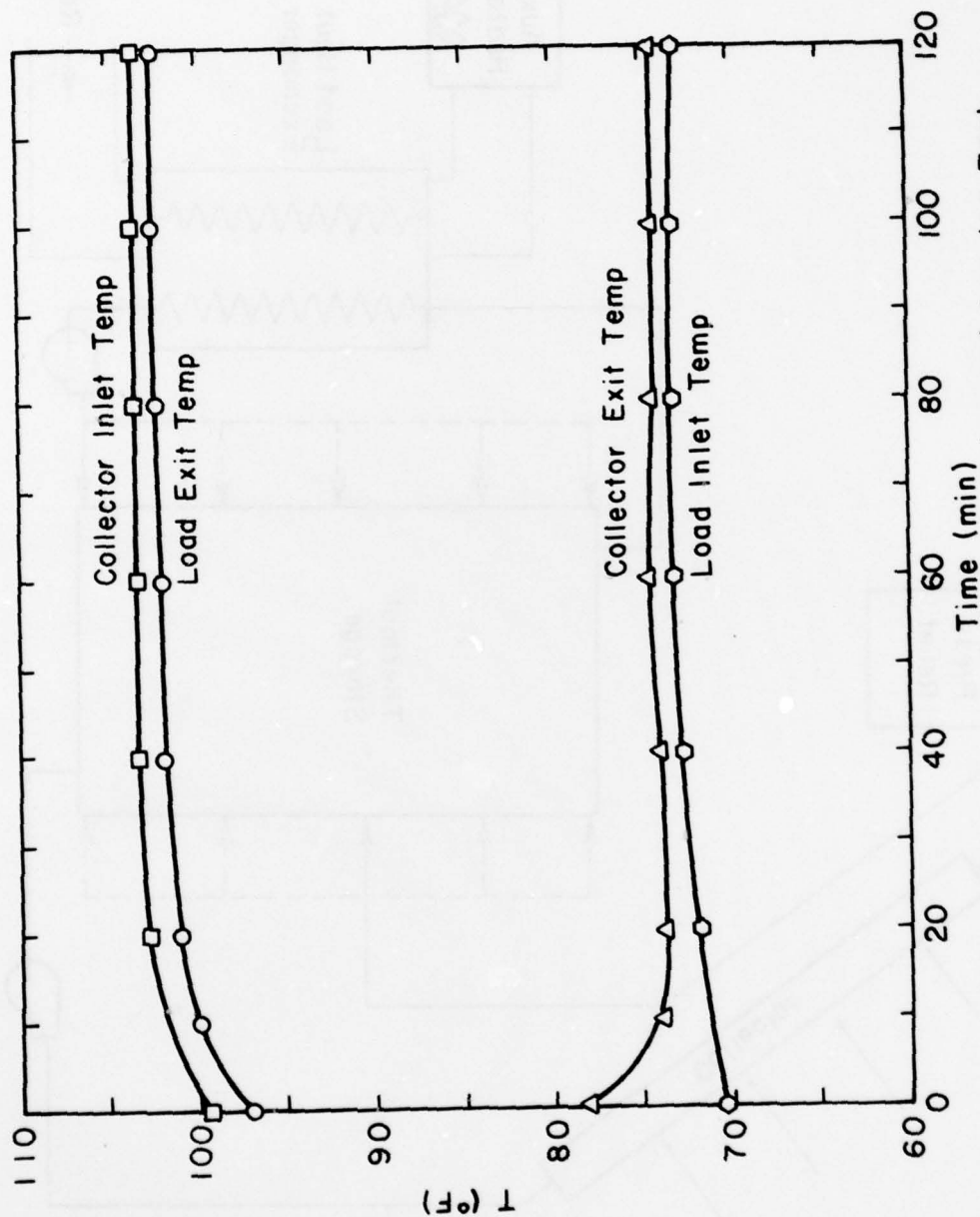


Fig. 23. Temperature Histories of Flows Entering and Leaving Tank During Simultaneous Charge and Discharge

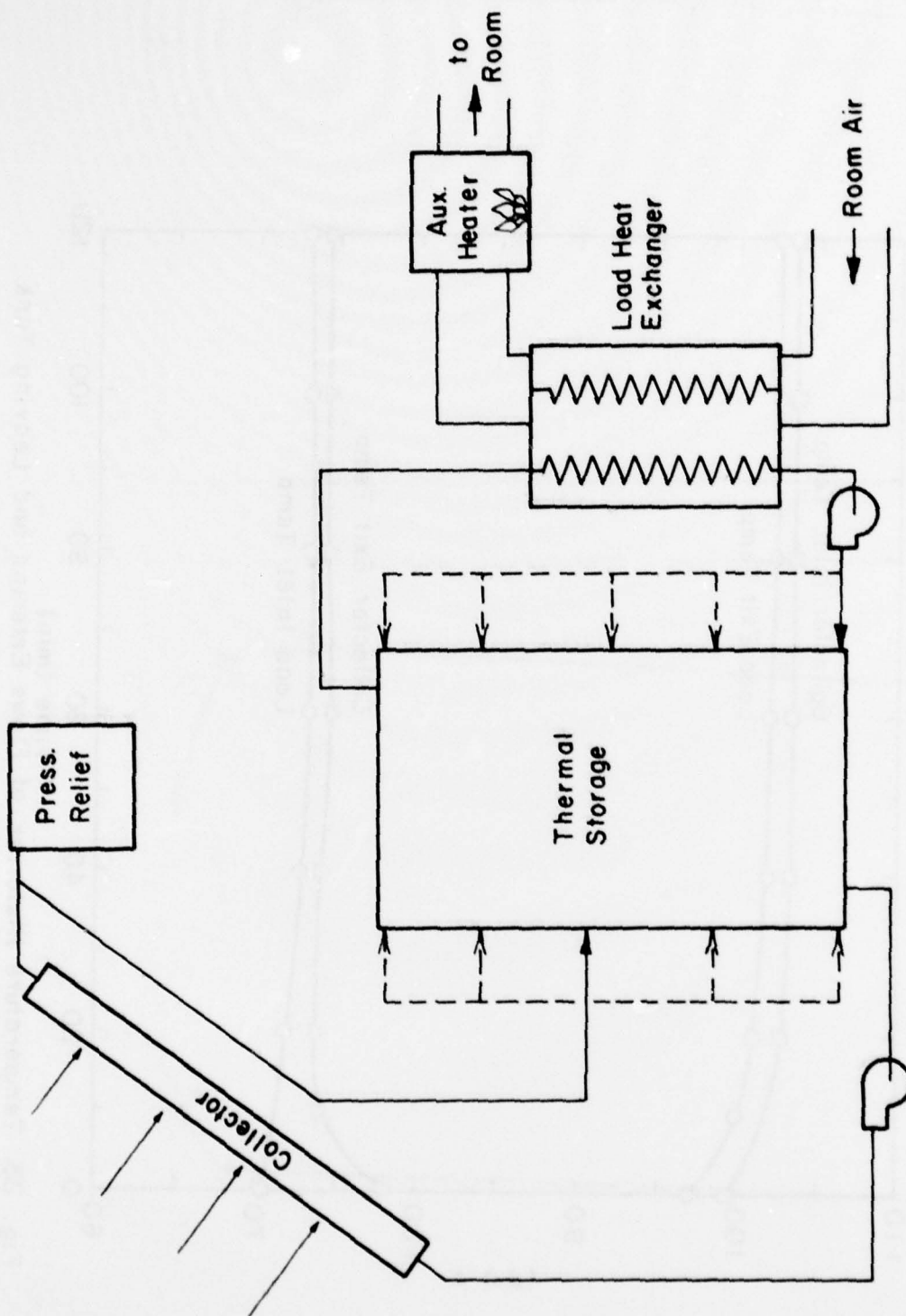


Fig. 24. System Configuration

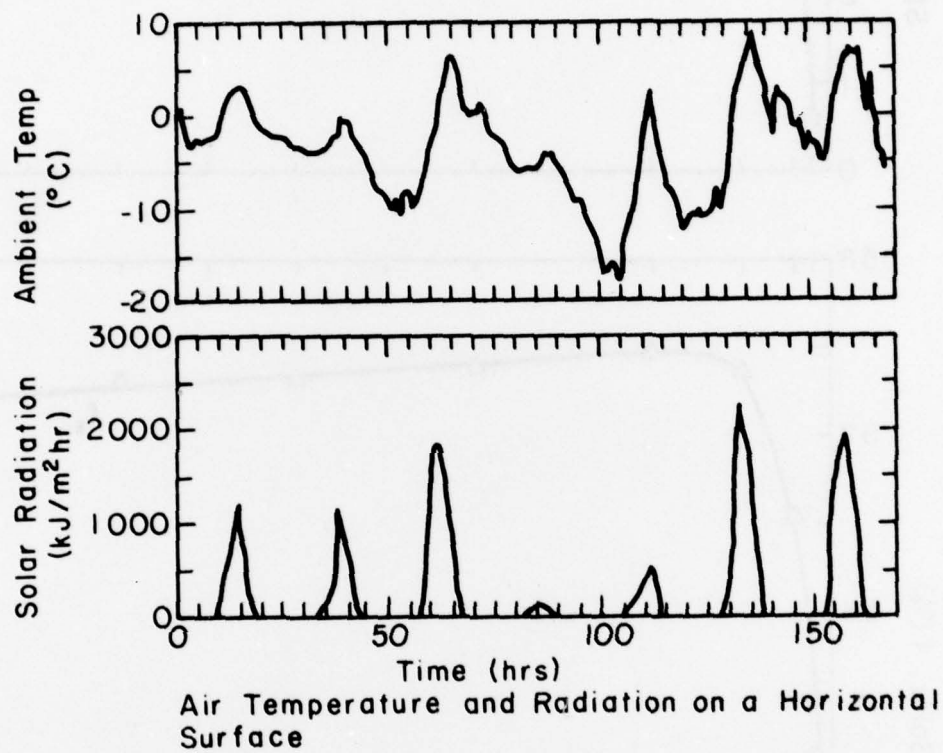


Fig. 25. Weather Data from Duffie and Beckman, Reference 9, Fig. 10.2.2.

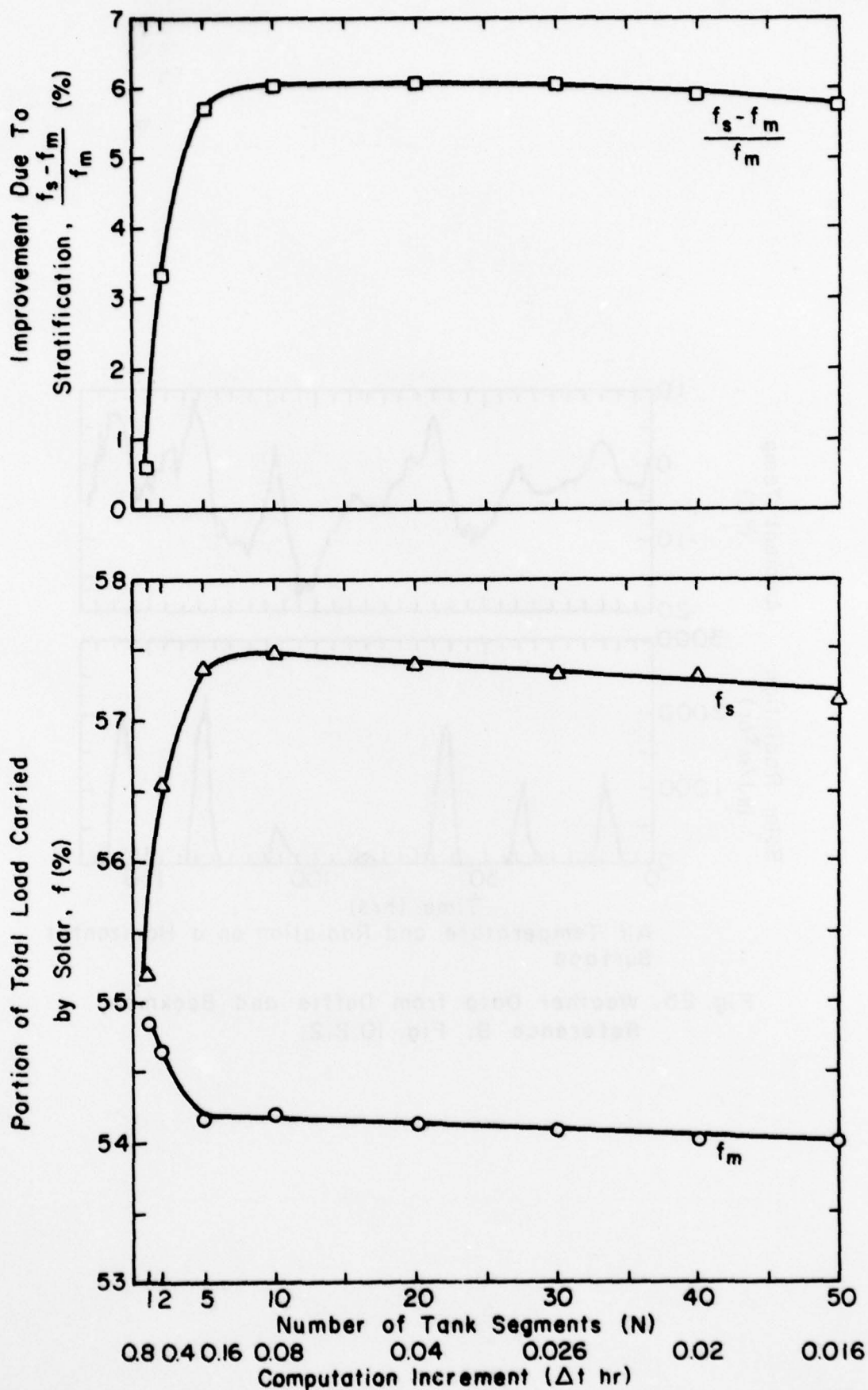


Fig. 26. Effect of Number of Tank Segments on Simulation Results

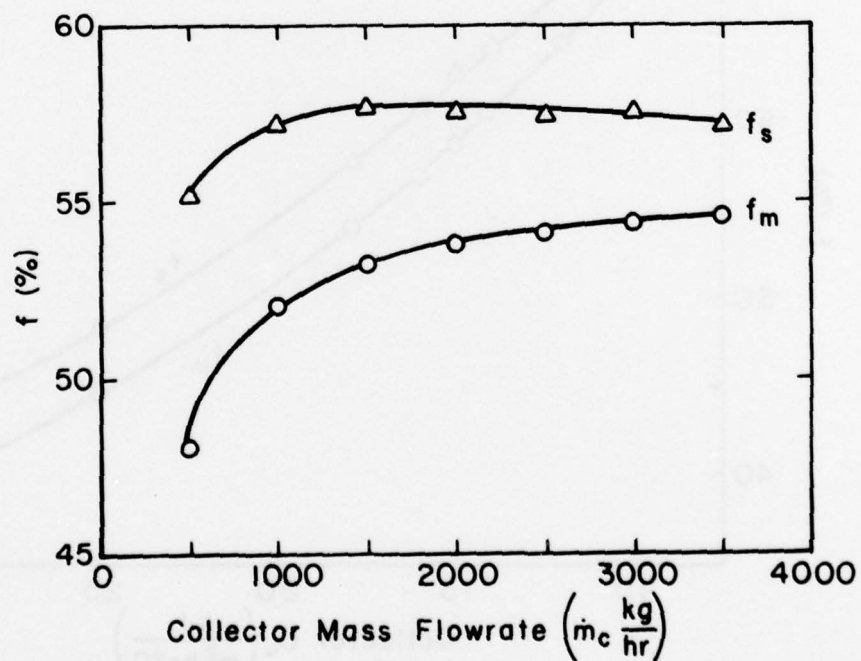
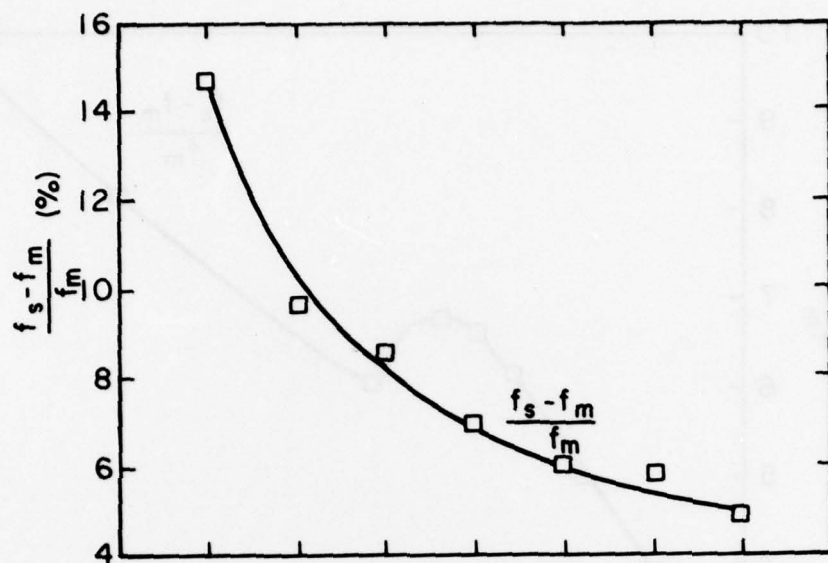


Fig. 27. Effect of Collector Mass Flowrate on System Performance

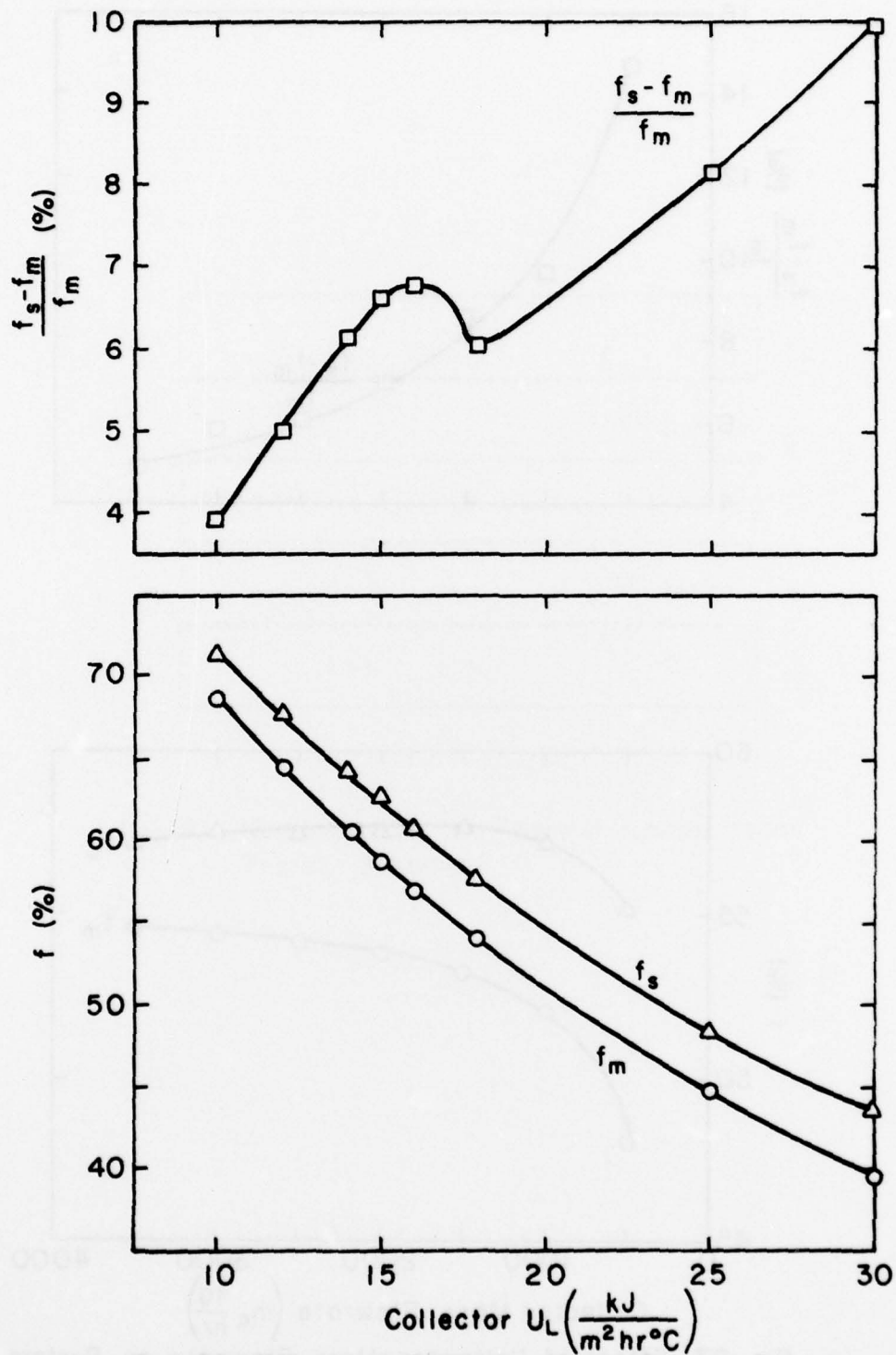


Fig. 28. Effect of Collector U_L on System Performance

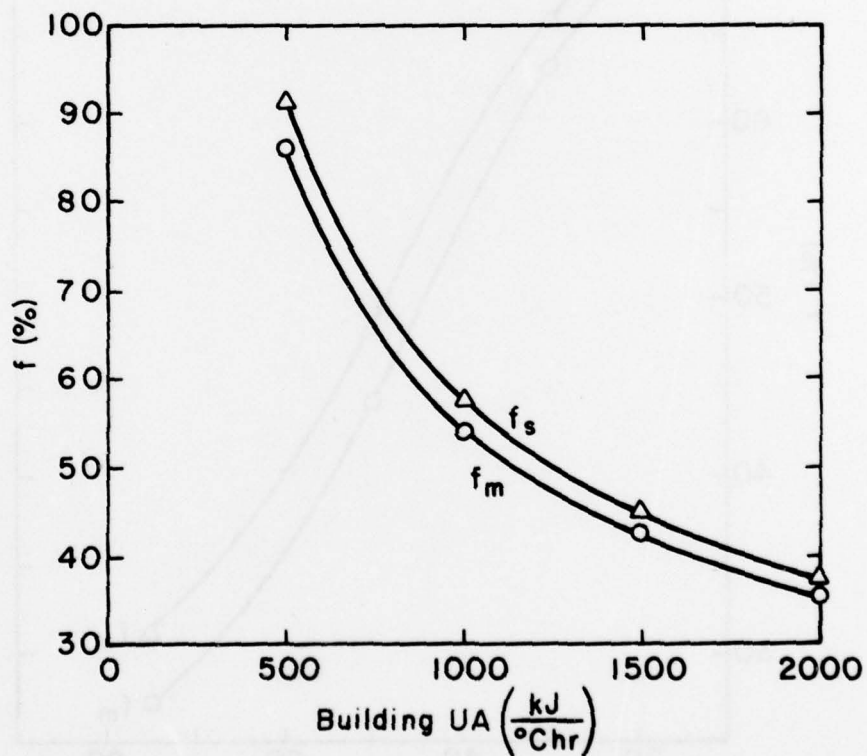
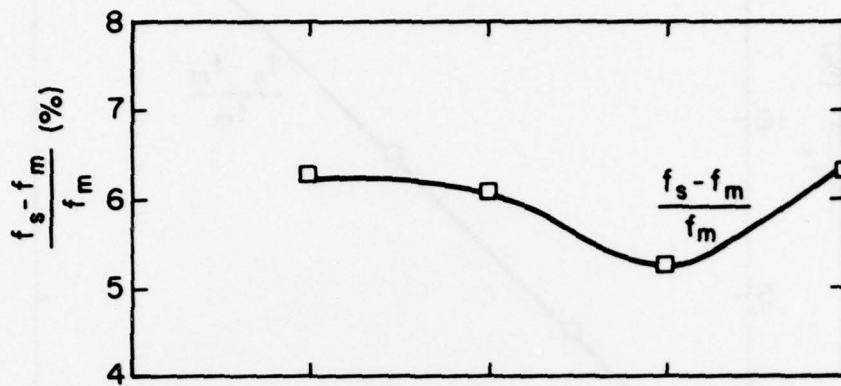


Fig. 29. Effect of Building UA on System Performance

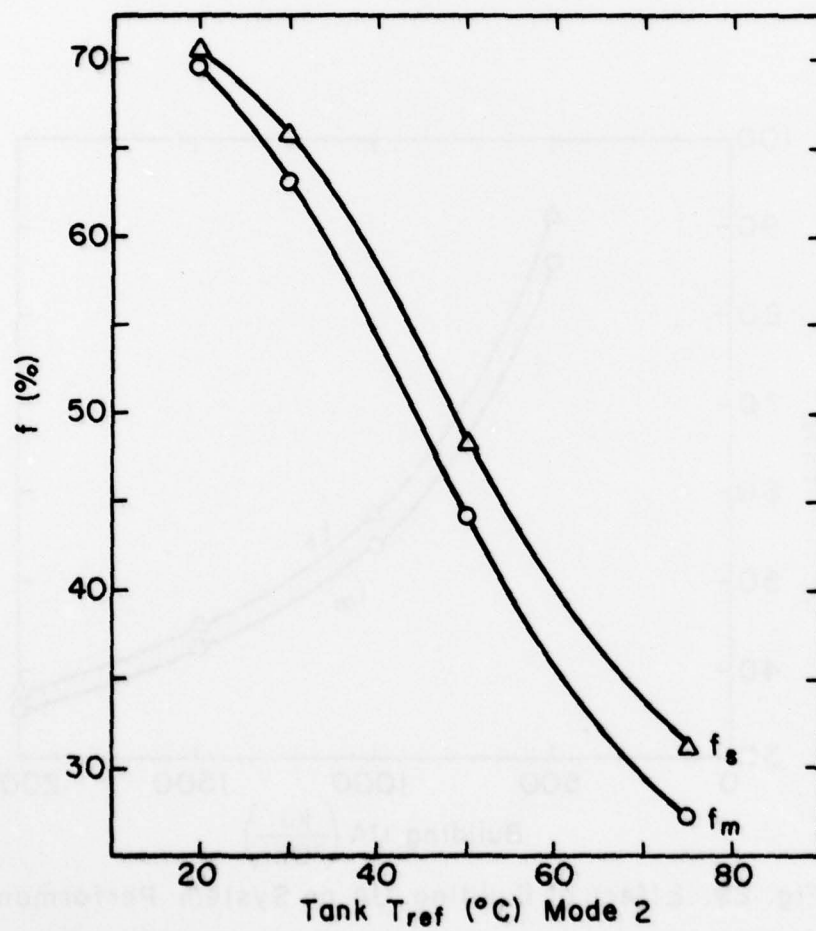
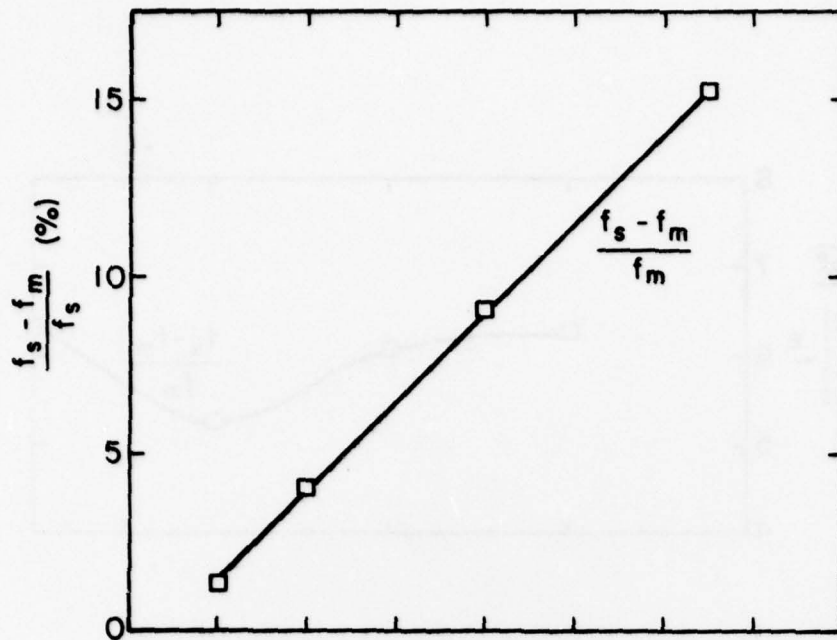


Fig. 30. Effect of Tank T_{ref} on System Performance

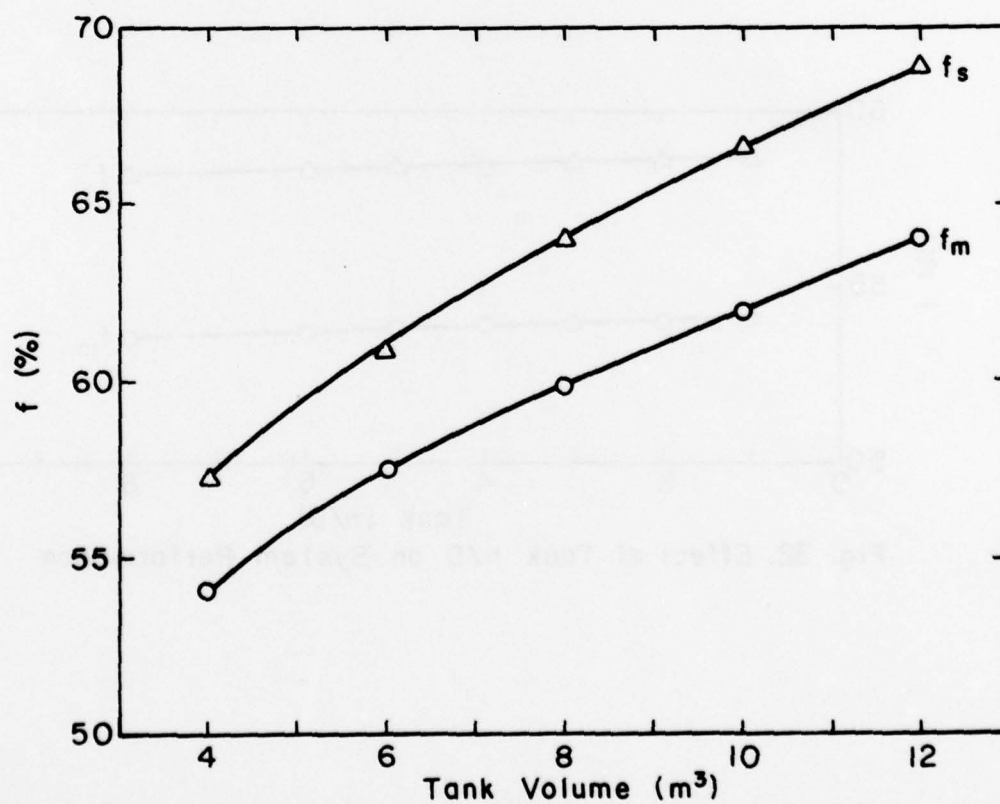
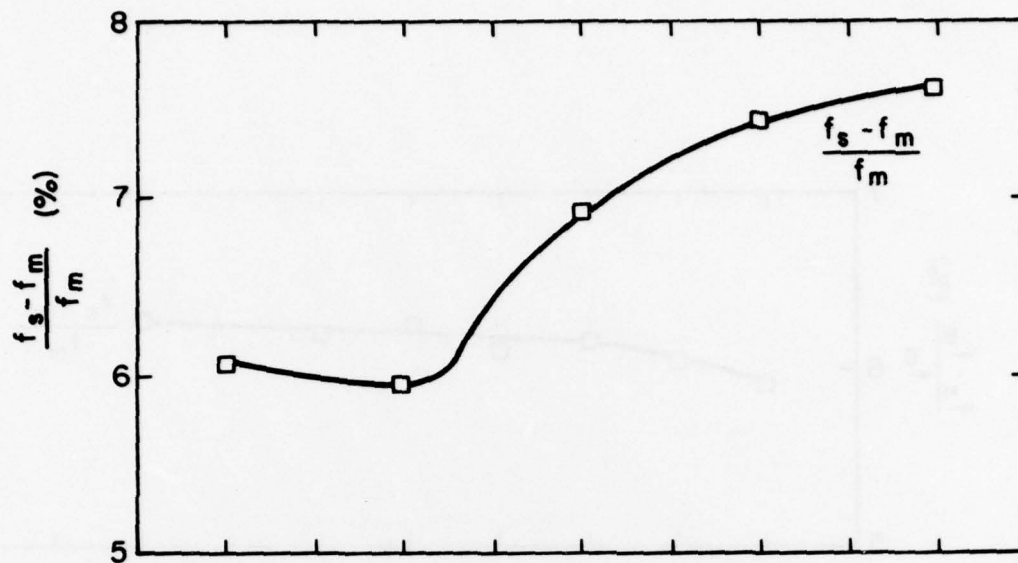


Fig. 31. Effect of Tank Volume on System Performance

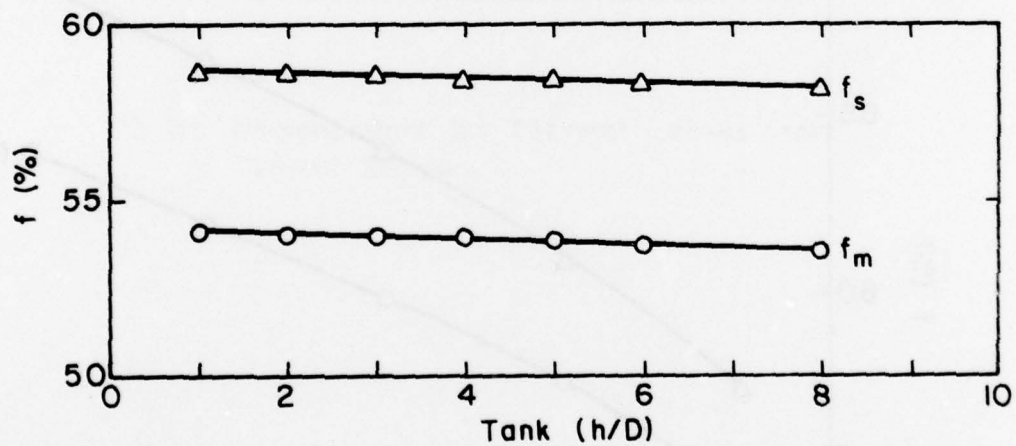
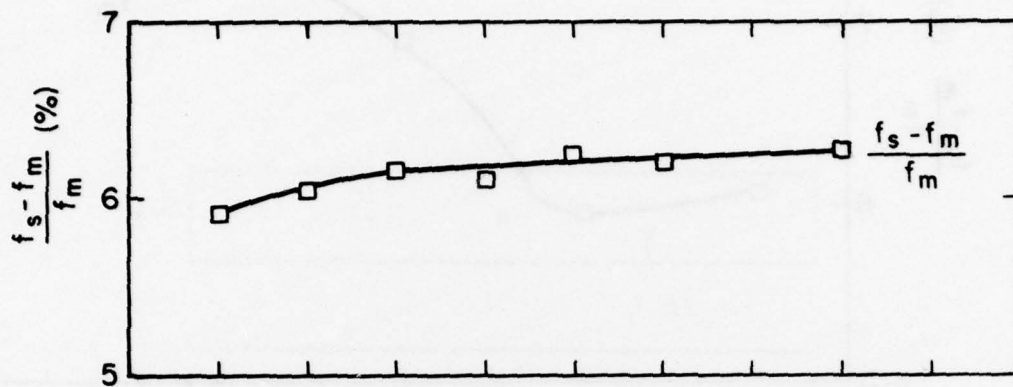


Fig. 32. Effect of Tank h/D on System Performance

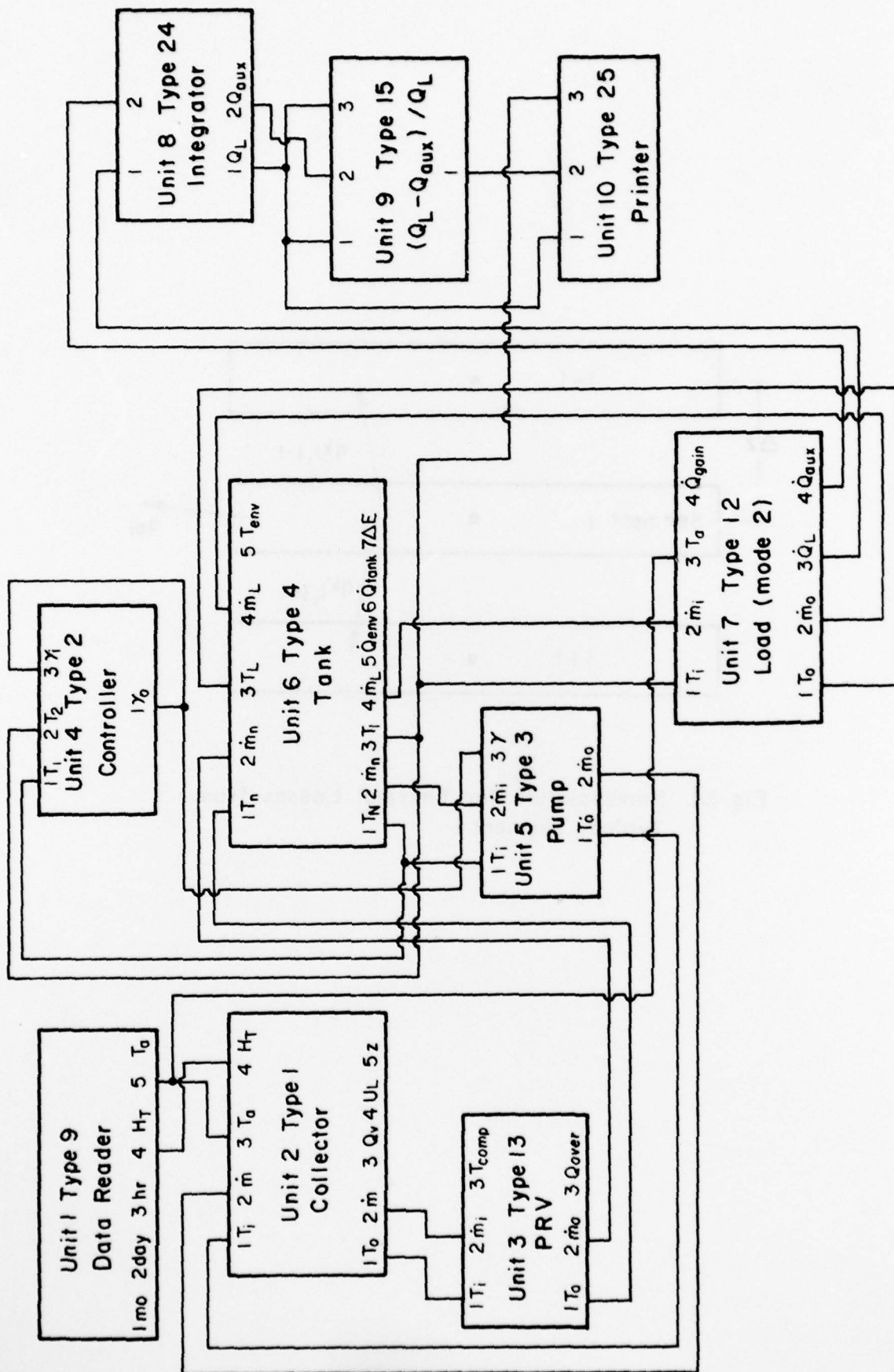


Fig. 33. TRNSYS Information Flow Diagram

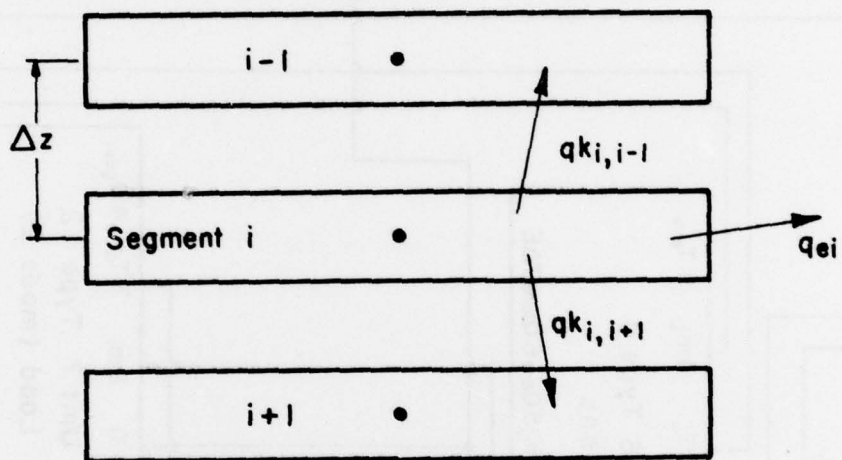


Fig. B1. Nomenclature for Thermal Losses from Typical Segment i

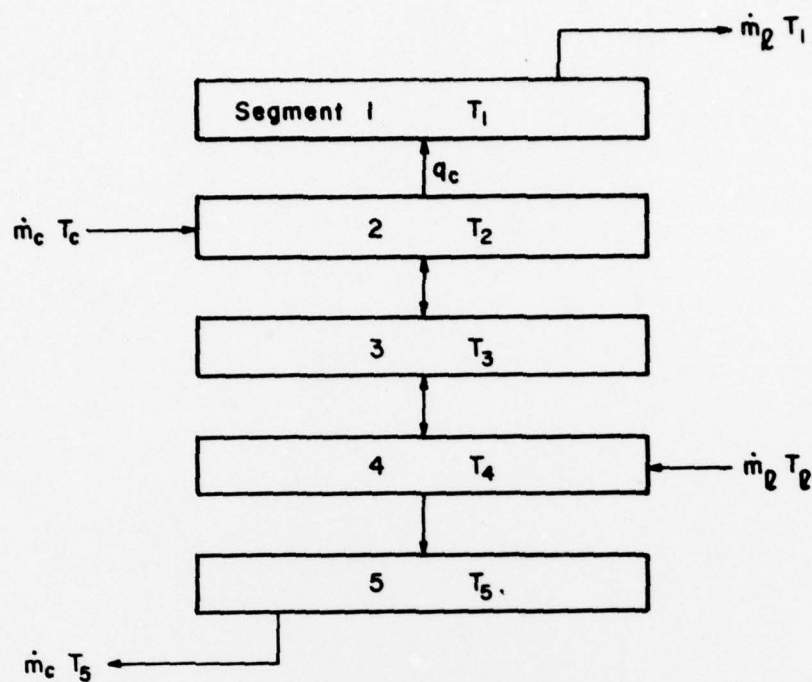


Fig. B2. Example of Tank Segment Configuration

Segment	$\dot{m}_l \geq \dot{m}_c$	$\dot{m}_c \geq \dot{m}_l$
1	$\dot{m}_l c_p (T_2 - T_1)$	$\dot{m}_l c_p (T_2 - T_1)$
2	$\dot{m}_c c_p T_c - \dot{m}_l c_p T_2 + (\dot{m}_l - \dot{m}_c) c_p T_3$	$\dot{m}_c c_p T_c - \dot{m}_l c_p T_2 - (\dot{m}_c - \dot{m}_l) c_p T_2$
3	$(\dot{m}_l - \dot{m}_c) c_p (T_4 - T_3)$	$(\dot{m}_c - \dot{m}_l) c_p (T_2 - T_3)$
4	$\dot{m}_l c_p T_l - \dot{m}_c c_p T_4 - (\dot{m}_l - \dot{m}_c) c_p T_4$	$\dot{m}_l c_p T_l - \dot{m}_c c_p T_4 - (\dot{m}_c - \dot{m}_l) c_p T_3$
5	$\dot{m}_c c_p (T_4 - T_5)$	$\dot{m}_c c_p (T_4 - T_5)$

Table B1. q_c , Convective Energy Transfer to each Segment for Configuration shown in Fig. B2.